1966

Transonic turbine test rig exhauster system tests and tests of a reaction turbine.

Naviaux, Jacques Calvert.

TRANSONIC TURBINE TEST RIG EXHAUSTER SYSTEM TESTS AND TESTS OF A REACTION TURBINE

JACQUES CALVERT NAVIAUX

TRANSONIC TURBINE TEST RIG EXHAUSTER SYSTEM TESTS

AND

TESTS OF A REACTION TURBINE

by

Jacques Calvert Naviaux
Captain, United States Marine Corps
B.S., United States Naval Academy, 1959

Submitted in partial fulfillment
of the requirements
for the degree of

MASTER OF SCIENCE IN AERONAUTICAL ENGINEERING

from the

UNITED STATES NAVAL POSTGRADUATE SCHOOL
December 1966

ABSTRACT

The primary purpose of the Exhauster System of the Transonic Turbine Test Rig of the United States Naval Postgraduate School, Monterey, California, is to increase the range of turbine operating pressure ratios by maintaining a partial vacuum inside a hood that encloses the turbine. The first part of this study is concerned with the design and the tests of the exhauster system. The experiments were used to establish a method of predicting the operating characteristics of similar ejectors which is based on the universal ejection properties of turbulent jets.

The second part of this study describes turbine tests utilizing the exhauster system that were carried out to investigate the effects of high values of the isentropic head coefficient and Reynolds number on the turbine performance. No correlation could be established between turbine Reynolds number and performance in the range tested.

TABLE OF CONTENTS

TABLE OF ILLUSTRATIONS

LIST OF TABLES

Table of Symbols

Symbols

A	Cross-sectional area (in^2 or ft^2)
c_p	Specific heat at constant pressure (BTU/lbm-^oR)
D	Diameter (in)
F	Impulse function, $PA + \rho AV^2$ (lbs)
g	Universal gravitational constant (32.174 lbm - ft/lb-sec^2)
G	Gas discharge, ρAV (lbm/sec)
HP	Horsepower
J	Conversion factor (778.16 ft-lb/BTU)
K_{is}	Head coefficient, isentropic (dimensionless)
n	Polytropic exponent (dimensionless)
N	Rotational speed, RPM
P	Pressures (psia)
R	Gas constant for air (53.345 ft-lb/lbm-^oR)
RE	Reynolds number (dimensionless) based on flow rate
RT	Reynolds number (dimensionless) based on rotor tip speed
r	Radius, inches
T	Temperature (^oR)
u	Instantaneous velocity in the x direction (ft/sec)
v	Instantaneous velocity in the y direction (ft/sec)
$\dot{W}$	Flow rate (lbm/sec)
X	Longitudinal coordinate (ft. or inches)
Y_1	Flow nozzle expansion factor (dimensionless)
γ	Specific heat ratio, c_p/c_v (dimensionless)
η	Efficiency (dimensionless)
ρ	Density (lbm/ft^3)

Φ Non-dimensional flow function

δ Referred pressure P_{to}/P_{std}, P_{std} = 14.7 psia (dimensionless)

Θ Referred temperature, T_{to}/T_{std}, T_{std} = 518.4 ^{o}R (dimensionless)

Subscripts

a Standard jet

AMB Ambient conditions

i Arbitrary jet

m Centerline velocity

o Characteristic of the jet

T Total pressure or temperature

∞ Existing in the undisturbed part of the flow

Superscripts

o Ratio between the surrounding fluid and the jet

Part I

TTR Exhauster System Tests

1. Introduction

The Transonic Turbine Test Rig installed at the Propulsion Laboratory of the Department of Aeronautics, U.S. Naval Postgraduate School, Monterey, California, receives its air supply from an Allis-Chalmers VA 312 compressor. The maximum turbine inlet total pressure attainable from the compressor is about 43 psia. In order to increase the range of possible operating pressure ratios with the existing air supply, the turbine is enclosed in a hood which is partially evacuated by the exhauster system. Since the turbine can only utilize a small portion of the mass flow from the air supply, the remainder can be used to drive the exhauster.

Very little design information is available on supersonic ejectors. The first part of this thesis is concerned with the evaluation of the design and performance of the exhauster system, and an investigation of the phenomena associated with a bounded, supersonic jet.

Funds for designing and building the Transonic Turbine Test Rig (TTR) were furnished by the Bureau of Naval Weapons (RAPP-14). Greatly appreciated advice and counsel was provided by Professor M.H. Vavra. Mr. L.T. Clark of the Department of Aeronautics furnished a great deal of advice and assistance in performing experiments.

2. Installation

Exhauster Installation

The complete TTR and exhauster installation is covered in detail by Eckert. [5] To test the exhauster separately from the turbine, a dummy exhauster hood was constructed for this purpose and secondary air was taken in from the atmosphere through a standard orifice installation. The standard orifice installation described by Eckert was

equipped with a bellmouth on the intake side and a diffuser at the hood entrance. [4] Figure 1 shows a schematic of the secondary air flow installation.

In addition to the static pressure taps installed in the exhauster and described by Eckert, Kiel probes were installed in the nozzle plenum chamber and secondary air inlet pipe (Figure 1). [5] Static pressure tap station designations are given in Figure 1. All pressures were measured in inches of mercury against atmospheric pressure as a reference, using 96 inch manometers with .01 inch graduations, except for the driving-nozzle total pressure which was measured on a precision gauge graduated in increments of .05 lbs/square inch. Secondary flow rate differential pressures at the metering orifice were measured in centimeters of mercury on a micro-manometer graduated in increments of .01 cm. Total temperature readings were measured with standard I.C. thermocouples using an ice bath as a reference.

3. Exhauster-Only Tests

General

Initially the nozzle total pressure was held constant while the gate valve (Figure 1) was used to vary secondary flow rates. Runs were made with the nozzle total pressure set at 20, 25, 30, and 35 psia. Then with the gate valve (Figure 1) fully open, nozzle total pressure was varied from 2 psig to the maximum obtainable from the Allis-Chalmers compressor in increments of 2 psig. Flow rate measurements from the standard orifice, nozzle total pressure and temperature, and static pressure readings were taken at each operating condition. In order to minimize the temperature difference between the primary and secondary flows, the Allis-Chalmers aftercooler was run at the full

cold setting, giving a temperature difference of about 20 degrees Fahrenheit between the primary and secondary air. The tests were then repeated with one 40 inch long section of the mixing tube removed.

Since the nozzle cannot accommodate the full flow rate of the Allis-Chalmers compressor, it was necessary to throttle the compressor flow, discharging a portion of it to the atmosphere. The maximum total pressure obtainable at the driving-nozzle was limited by approaching temperature and surge limits on the compressor. A six foot flexible pipe connection between the driving-nozzle and air supply (Figure 1) produced an unexpectedly large pressure loss (about 8 psig static pressure) limiting the nozzle total pressure to a maximum of 36 psia.

The entire system was allowed to stabilize before taking readings at each point of operation. The system was very stable except at high secondary flow rates, where the static pressures at stations one through four showed a large low frequency variation of as much as 2 inches of mercury. However, this instability was not reflected in the total pressure maintained inside the hood. The instability in the mixing tube at high flow rates is contrary to both experimental evidence and theory given by Alexander, Baron, and Comings. [3] These authors found that the instability in the mixing tube occurred at zero secondary flow rates and hypothesized that this was due to the natural function of the jet in entraining air from its surroundings, requiring a reverse flow eddy in the absence of any secondary flow. At zero secondary flow rates, the TTR exhauster system was very stable, even at the maximum driving nozzle total pressure ratio. It is possible that hood leakage may have furnished a slight amount of secondary flow to stabilize the jet at zero secondary flow rates, although no evidence of any leakage was detected.

The first attempt to obtain velocity profiles was made with a W-157 probe built by the United Sensor Corporation, East Hartford, Conn., which is a wedge shaped probe with an included angle of about 34 degrees. The probe has a total pressure tap located in a small cut-out section and static pressure taps located on the face of the wedge. A mercury manometer was used to set the probe to a zero yaw angle by equalizing the static pressures from the two face taps.

Although it was realized that the detached shock Mach number for the wedge would be above the Mach numbers encountered in the flow, it was hoped that a calibration curve could be obtained over the Mach number range of interest (.7 to 1.9). The supersonic wind tunnel with variable Mach numbers available at the U.S. Naval Postgraduate School is an AMRAD Model W-4 miniature blowdown tunnel. Since the physical dimensions of the probe precluded use of the actual probe for any calibration work, a full scale model of the probe tip complete with total and static pressure taps was constructed so that it could be mounted in the tunnel. Attempts to calibrate the probe on two occasions were completely futile since none of the readings obtained were repeatable within a tolerance of $\pm$ 50 percent.

Flow over the wedge was examined visually by means of a Schlieren system but failed to show any unusual conditions which might have accounted for the wide variations in dynamic pressure. It is possible that the tunnel calibration curves are inaccurate or that repeatable Mach numbers cannot be obtained with the tunnel. The probe was tested for leaks, and none were found upon completion of testing.

While waiting for the construction of the probe model, velocity traverses were taken with the W-157 probe with the concept that flow

yaw angles could be checked even if the probe could not be calibrated. No evidence of any large swirl components was found since the yaw angles did not exceed 5 degrees and were usually less than 1 degree. However, upon completion of the traverses, it was found that the W-157 probe had developed a leak between the total and one static tap; therefore, no conclusions can be based upon data obtained with this probe.

The next attempt to take velocity traverses was made with a pitot-static tube 1/16 inch in diameter mounted on a $\frac{1}{4}$ inch stainless steel tube. This tube produced very erratic readings attributable to severe probe vibration. Since the probe did indicate a very unsymmetrical flow pattern, this possibility was checked by reading static pressures from one orifice at a time at each station. All of the pressure taps produced readings within .05 inches of mercury of each other showing no indication of unsymmetrical flow.

Since the difficulties seemed to be due to probe vibration, a total head probe (Figure 2) was constructed so that it could be supported from both ends. The idea of constructing a pitot-static probe was discarded initially, since the holes through which the probe had to be inserted were too small for a static probe with the orifices located far enough back of the tip to conform to standard practice (eight to ten diameters). Therefore, it was assumed that the static pressure was uniform across the section and total head traverses were made only. The total head traverse at station one indicated a lower total pressure at the centerline than at the off-center stations. Since this phenomena was not expected at the time, a small non-standard static probe was constructed anyway (Figure 2) to take static traverses. The velocity profiles shown in Figures 3 to 5 were obtained with these measurements.

No attempt was made to calibrate the probes due to lack of facilities. In addition, the probes could not be inserted or withdrawn while the system was in operation without damage to the probe, so that a slightly different equilibrium point was attained for each station.

Data Reduction

Secondary flow rates were measured by the orifice installation in the secondary flow inlet. Calculation of flow rates was accomplished by computer program based on the orifice formulas used by Eckert.[4] Agreement of flow rates calculated from vena contracta and flange tap differential pressures were within 2 percent for all flow rates and generally within 1 percent or less.

Nozzle flow rates were calculated from assumed polytropic exponents and measured values of nozzle total temperature and pressure. Calculations for nozzle flow rates in the subsonic region utilized isentropic flow and one-dimensional normal shock relations.

The velocity profile data reduction was accomplished by means of a computer program using the Rayleigh formula, with the known local static and total pressure behind the shock. Standard compressible flow relations were used for subsonic velocities.

4. Exhauster Performance

General

The classical method of analysis is based on a one-dimensional momentum analysis; however, if nothing is known about the secondary flow except its initial total pressure and temperature, the problem cannot be solved since the number of unknown quantities exceeds the number of independent flow equations that can be formulated. Therefore, it became necessary to find an additional relationship between

the primary and secondary flow rates.

Of all the various approaches dealing with the problem of turbulent jets, the one that appeared to have the greatest potential is a hypothesis set forth by O. V. Yakovlevskii. [14] His hypothesis, based on a wide survey of experimental and theoretical data, is that in the discharge of a gas jet, the ejection properties are the same as those of a geometrically similar submerged jet of an incompressible fluid with the same initial impulse. A submerged jet is defined as a free jet discharging into a fluid at rest. This hypothesis leads to the concept of the universality of the ejection properties of a turbulent jet regardless of the conditions of discharge.

Assuming that the basic property of a jet is its impulse, and that the basic characteristic of such a jet is the ejection or entrainment of mass from the surrounding media, an arbitrary jet and a standard, isothermal, submerged free jet discharging from geometrically identical nozzles with identical impulses in the initial cross section should have similar ejection properties.

The basic part of Yakovlevskii's analysis is presented here as a basis for further development, retaining the author's notation:

Restating the basic hypothesis in mathematical form,

$$\frac{dG_i}{dx} = \frac{dG_a}{dx} \tag{1}$$

where:

G = gas discharge, ρVA in the initial cross section

x = longitudinal coordinate in the direction of flow

i = index referring to an arbitrary jet

a = index referring to a standard, submerged, isothermal jet

Then, the relationship between the standard jet and the arbitrary jet is expressed by the ratio,

$$\frac{G_a}{G_i} = \sqrt{\frac{\rho_a}{\rho_i}} = \sqrt{\rho^\circ} \tag{2}$$

where ρ_a is the density of the surrounding medium and ρ° is the density ratio. Let:

$$G^\circ = \frac{G}{G_o} \tag{3}$$

where G_o is the gas discharge at the initial cross section and,

$$x^\circ = \frac{x}{r_o} \tag{4}$$

where r_o is the initial radius of an axisymmetrical jet. Eq. (2) can now be written in a non-dimensional form:

$$\frac{dG_i^\circ}{dx^\circ} = \sqrt{\rho^\circ}\ \frac{dG_a^\circ}{dx^\circ} \tag{5}$$

This hypothesis amounts to the assumption of the universality of transverse and longitudinal velocity profiles.

It is shown by Yakovlevskii that the increase in flow rate in some arbitrary section of the submerged jet (Figure 6) is, [14]

$$dG = 2\pi \rho_\infty V_\infty r\, dx \tag{6}$$

where:

ρ_∞ = density in the undisturbed part of the flow

V_∞ = instantaneous velocity in the y direction in the undisturbed part of the flow

Putting Eq. (6) into a non-dimensional form,

$$\frac{dG^\circ}{dx^\circ} = 2\,\frac{r}{r_o}\,\frac{U_m}{U_o}\,\rho^\circ\,\frac{V_\infty}{U_m} \tag{7}$$

where:

$\rho^\circ = \frac{\rho_\infty}{\rho_o}$ = the ratio of the density of the undisturbed portion of the surrounding flow to the density of the jet

r = radius at some arbitrary point of the jet

U_m = instantaneous centerline velocity in the x direction

U_∞ = instantaneous velocity in the x direction in the undisturbed part of the flow

U_o = instantaneous velocity in the x direction of the jet discharge

He goes on to state that the following relationship is valid for this case:

$$\frac{r\,U_m}{r_o\,U_o} = \frac{1}{\sqrt{\rho^\circ}\,\Phi\left(\frac{U_m}{U_o}, \rho^\circ\right)} \tag{8}$$

and that for small values of ρ°, Φ is a constant. Thus,

$$\frac{dG^\circ}{dx^\circ} = \frac{1}{\sqrt{\rho^\circ}} = \text{const}\ \frac{V_\infty}{U_m} \tag{9}$$

Then, using Eq. (7) he gives the formula for the initial cross-section of an axisymmetric jet as,

$$G^\circ = \sqrt{\rho^\circ}\ \alpha_1 \left(x^\circ + \beta_1\right) \tag{10}$$

where α_1 and β_1 are experimentally determined constants. The following values are given by Yakovlevskii for the case of an incompressible submerged free jet: [14]

α_1 = 0.11 to 0.20

β_1 = -4.3

The minus sign attached to α_1 is due to the Russian practice of basing jet coefficients on the assumption that the jet is issuing from a point source located at some distance in front of the nozzle, as Eq. (10) becomes meaningless near the nozzle. Taking the optimum length of the mixing tube as 8.5 nozzle diameters, an average of the commonly used

value of 7 to 10 diameters, and taking α_1 as 0.115, there is for an assumed value of $\sqrt{\frac{\rho}{\rho_o}}$ of unity,

$$G^\circ = \frac{G}{G_o} = 0.115\left(\frac{4.76 \times 8.5}{4.76/2} - 4.3\right) = 1.476 \tag{11}$$

where:

4.76 = driving nozzle diameter (inches)

8.5 = optimum length of mixing tube (driving nozzle diameters), taken as the value for x

4.76/2 = initial radius of the axisymmetrical jet, r_o (inches)

In actuality, $\sqrt{\frac{\rho}{\rho_o}}$ varied from about 1.2 to 0.96 for the present tests.

The optimum length chosen for the mixing tube was verified by removing one 40 inch section of the mixing tube. The tests showed that almost identical operating characteristics were obtained for the 40 and 80 inch long tubes. Comparing the coefficient of discharge of Eq. (11) with the experimental values of the present data (Table I) shows very good agreement between the two provided that a suitable choice is made for α_1. However, on the basis of information available, and due to the wide variation of α_1 from author to author, the arbitrary choice of α_1 to fit experimental data cannot be defended. It is noteworthy though that the term G^o is nearly a constant throughout the entire range of operation up to the point of secondary flow choking. Therefore, an attempt was made to place the flow relationship of Eq. (10) on a firmer basis. Using the standard definition of impulse function,

$$F = PA + \rho AV^2 \tag{13}$$

the nozzle impulse function was plotted versus $\sqrt{\frac{\rho}{\rho_o}}$ where ρ_o is the density of the nozzle discharge. Figure 7 shows that $\sqrt{\frac{\rho}{\rho_o}}$ is a linear function of the nozzle impulse function. If the impulse function is

plotted versus the secondary flow rate (Figure 8), a linear relationship is evident up to the point of secondary flow choking, and thus the secondary flow rate for this particular system at a given nozzle impulse can be determined from Figure 8 for unchoked secondary flow. The linear relation holds only for the case where the nozzle discharge is supersonic. Since the geometry of the nozzle is fixed, there was no way to test the generality of the coefficient of discharge determined from Figure 8; however, since the basic hypothesis appears to be true, it should provide a reasonable first approximation for a geometrically similar system.

The reason that the linear relationship between the nozzle impulse function and the secondary flow rate does not hold for the subsonic case is probably due to the fact that one-dimensional isentropic and normal shock relations were used to calculate nozzle exit conditions, and these are not truly representative of the actual flow phenomena.

The next problem was to find some means of determining the required mixing tube length. Since the original hypothesis was based on the assumed universality of velocity profiles, it was assumed that a determination of the necessary length of the mixing tube could be based on incompressible flow. However, even with this simplification, the problem was not tractable due to the presence of a longitudinal pressure gradient (Figures 9, 10) and the problems associated with turbulent flow. Therefore, an empirical approximation was sought.

Viktorin carried out a series of experiments in 1941 using water as the driven and driving fluid. [12] His experimentation was based on an earlier theoretical analysis performed by Flugel. Viktorin found

that the velocity distribution in the mixing chamber behaved in the same fashion as a circular wake with the width proportional to about $x^{1/3}$ and the centerline velocity proportional to about $x^{-2/3}$. The assumption is made that the mixing process reaches an optimum point when the core of the jet contacts the mixing tube, and that any further increase in mixing tube length will result in a trade off between increased mass flow rate and increased mixing and frictional losses. Assuming that the primary fluid emanates from a point source located at some point upstream of the nozzle in order to find a constant of proportionality, it was determined that the mixing process would reach an optimum state about 40 inches downstream of the nozzle. This was verified by the performance data (Figures 12, 13 and 14) for the system with one 40 inch section of the mixing tube removed.

A comparison of predicted centerline velocities with experimental data (Table II) shows that the predicted values are within 10% of the experimental values for stations two through four. The discrepancy at station six can be attributed to the fact that at this point the flow is completely mixed and is now characteristic of turbulent flow in a pipe. It is thought that the flow at station one differs from the predicted value due to off-design operation of the nozzle, i.e., the nozzle discharge static pressure is greater than the receiver static pressure, and the nozzle never reached the design point during the experimentation. Examination of the total pressure traverse shows that the maximum total pressure was not obtained on the axis of the jet. This matches experimental data given by Abramovich. [1] He shows that the jet actually has a small subsonic region along the centerline and that the centerline total pressure is less than the off-axis total

pressure until the flow has become sufficiently adjusted to become isobaric.

The analysis up to this point has considered only the case of unchoked secondary flow. As is evident from Figure 12, the secondary flow rate becomes almost independent of the nozzle total pressure above a pressure ratio of 2.3. A supersonic ejector has two regions of operation. One region, the so-called mixed region occurs when the driving-nozzle total pressure ratio is sufficiently low to make the ejector flow dependent on the back pressure. If the driving-nozzle pressure ratio is increased sufficiently, the flow will become independent of the back pressure, since it becomes supersonic. As the nozzle pressure ratio is increased even further, the secondary flow will eventually choke at the point of minimum area.

The supersonic region is characterized by the condition that the secondary flow static pressure at the driving nozzle exit plane is less than the nozzle exit static pressure. This point of operation was not reached with this particular system, and the system operates in the mixed region. However, since secondary flow choking does occur, the possibility of sonic flow at the minimum secondary flow area was checked over a wide range of nozzle pressure ratios, and it was found that the secondary flow does not choke at this point. Calculation of the polytropic exponent and the flow function (Equation 14) between the secondary flow inlet and the nozzle annulus (Table III) shows that at the higher flow rates, the process is nearly isothermal and that the flow function approaches the critical flow function (Equation 17) indicating choking at some point between the inlet and the nozzle annulus.

If the secondary flow is not restricted prior to reaching the

nozzle exit plane, flow characteristics can be found using a method developed by Fabri. [7] A more elaborate method utilizing the method of characteristics was presented by Addy. [2] Both of these methods are concerned with flow in the supersonic region. For flow in the mixed region, both authors use a form of the one-dimensional momentum analysis. However, as mentioned before, solution of the momentum equation depends on control of the secondary flow rate or pressure ratio.

The empirical method of determining the ejector pumping characteristics has some serious drawbacks as presented here. The coefficient of ejection which is based on empirical data is an unknown function of system geometry, and since the viscous effects have been ignored, it does not provide any means of predicting the pressure distribution in the mixing tube. Figures 9 and 10 show the mixing tube static pressure profiles. No theory could be developed to produce the mixing tube static pressure distribution.

Momentum Analysis

Once the values of secondary flow rate are determined from Eq. (10), a one-dimensional momentum analysis can be conducted to determine exhauster performance. The analysis was designed to parallel the preliminary design calculations by Vavra in order to determine the validity of the one-dimensional approach. [10] In order to simplify the equations, polytropic process relations as well as the non-dimensional flow function Φ were used throughout. These were taken from Vavra. [9]

For an expansion process,

$$(14)\quad \frac{\dot{W}\sqrt{T_{T_0}}}{A\,P_{T_0}}\sqrt{\frac{R}{g}} = \Phi = \sqrt{\frac{2\gamma}{\gamma-1}\left[\left(\frac{P}{P_{T_0}}\right)^{\frac{2}{n}} - \left(\frac{P}{P_{T_0}}\right)^{\frac{n+1}{n}}\right]}$$

where:

(15) $$n = \frac{\gamma}{1 - \eta_p(\gamma - 1)}$$

n = polytropic exponent

γ = ratio of specific heats

$\dot{W}$ = flow rate (lbm/sec)

T_{to} = inlet stagnation temp. (^oR)

A = flow area at station of interest (in^2)

P_{to} = inlet stagnation pressure (psia)

P = static pressure at station of interest (psia)

R = gas constant for air (ft lb/lbm ^oR)

g = universal gravitational constant (lbm-ft/lb-sec^2)

For a compression process,

(16) $$\frac{\dot{W}\sqrt{T_1}}{A P_1}\sqrt{\frac{R}{g}} = \Phi = \sqrt{\frac{2\gamma}{\gamma - 1}\left[\frac{T_{T1}}{T_1}\left(\frac{P_2}{P_1}\right)^{\frac{2}{n}} - \left(\frac{P_2}{P_1}\right)^{\frac{n+1}{n}}\right]}$$

where the subscripts 1 and 2 refer to the inlet and station of interest respectively. Figure 1 shows the exhauster with the station designations used in the analysis.

For the exhauster operating conditions the flow through the nozzle will be choked. For this condition, the flow function, $\bar{\Phi}$, becomes

(17) $$\bar{\Phi}_n = \left(\frac{2}{n+1}\right)^{\frac{1}{n+1}}\sqrt{\frac{2\gamma}{\gamma - 1}\left(\frac{n-1}{n+1}\right)}$$

It was assumed that the nozzle total pressure and temperature are known. Assuming a polytropic exponent for the flow in the nozzle to the throat, $\bar{\Phi}$ can be calculated. Then, another polytropic exponent was assumed from the throat to the nozzle exit so that,

(18) $$\bar{\Phi}_e = \bar{\Phi}_n \frac{A_N}{A_1}$$

Expressing the dimensionless flow function in terms of pressure ratios,

$$(19)\quad \Phi_e = \sqrt{\frac{2\gamma}{\gamma-1}\left[\left(\frac{P_{IN}}{P_{TN}}\right)^{\frac{2}{n}} - \left(\frac{P_{IN}}{P_{TN}}\right)^{\frac{n-1}{n}}\right]}$$

Since Φ_c is known from the choked flow condition, and P_{TN} and T_{TN} are known, it was possible to solve for P_{IN} by iteration. Having found P_{IN},

$$(20)\quad T_{IN} = T_{TN}\left(\frac{P_{IN}}{P_{TN}}\right)^{\frac{n-1}{n}}$$

$$(21)\quad V_{IN} = \sqrt{2gJc_p(T_{TN} - T_{IN})}$$

$$(22)\quad W_N = \Phi_e P_{TN} A_N \sqrt{\frac{g}{RT_{TN}}}$$

Thus the complete operating conditions have been determined for the driving nozzle. It was assumed that the air leaving the nozzle would undergo a full expansion without oblique shocks in order to continue with the solution. If the nozzle total pressure is low enough, the back pressure at the exit plane will be high enough to produce shocks in the nozzle with attendant subsonic flow at the nozzle exit. An investigation conducted on the experimental data showed that the flow from the nozzle would be independent of the back pressure whenever the nozzle total pressure exceeds 22 psia. Therefore, this particular analysis is only valid for nozzle total pressures above 22 psia.

Secondary air flow enters the flow measuring orifice with a total pressure, P_{TO}, and a total temperature, T_{TO}, equal to atmospheric conditions. Since the process is essentially adiabatic, T_{TO} will remain a constant. Then for the flow from the hood to the nozzle exit plane,

$$(23)\quad \frac{W\sqrt{T_{TO}}}{P_{TO}}\sqrt{\frac{R}{g}} = \Phi_d = \sqrt{\frac{2\gamma}{\gamma-1}\left[\left(\frac{P_{IT}}{P_{TO}}\right)^{\frac{2}{n_d}} - \left(\frac{P_{IT}}{P_{TO}}\right)^{\frac{n_d+1}{n_d}}\right]}$$

Because the weight rate of flow of secondary air is known for a given set of nozzle conditions, a ratio of P_{IT}/P_{TD} can be assumed, along with a value of P_{IT}. For this assumed pressure ratio,

$$T_{IT} = T_{TD}\left(\frac{P_{IT}}{P_{TD}}\right)^{\frac{n-1}{n}} \tag{24}$$

$$V_{IT} = \sqrt{2gJc_p(T_{TD} - T_{IT})} \tag{25}$$

Writing the momentum equation between stations 1 and 2, by assuming uniform velocity profiles, uniform static pressure distributions, and equal static pressures at the nozzle and secondary air discharges,

$$\left(\frac{W_N + W_T}{g}\right)V_{21} - \frac{W_N}{g}V_{IN} - \frac{W_T}{g}V_{IT} = A_{21}(P_{IN} - P_{21}) - Ff \tag{26}$$

The friction force Ff, was expressed as a pressure loss:

$$Ff = \frac{\pi}{4}D_2^2\,\Delta P = A_{21}\Delta P \tag{27}$$

where,

$$\Delta P = f\frac{L}{D_2}\frac{\bar{\rho}}{2}\bar{V}^2 \tag{28}$$

L = length of duct

D_2 = duct diameter

$\bar{V}$ = average velocity

$\bar{\rho}$ = average density

f = friction factor

f is a function of Reynolds number and pipe roughness. With an approximate range of Reynolds numbers from 1.7-2.2 x 10^5 and a surface roughness of .00015 for commercial steel pipe, a roughness to diameter ratio of .0024 was obtained. Entering a Moody diagram, a value of 0.017

for f was obtained. Then, a ΔP was calculated and subtracted from P_{IN} to obtain P^*.

Rewriting equation (26),

$$(29)\quad \left(\frac{W_N + W_T}{g}\right) V_{21} - \frac{W_N}{g} V_{IN} - \frac{W_T V_{IT}}{g} = A_{21}\left(P^* - P_{21}\right)$$

The total temperature after mixing was taken as a weighted average:

$$(30)\quad T_{T2} = \frac{W_T T_{TD} + W_N T_{TN}}{W_N + W_T}$$

With $W_N + W_T = W$ and writing the continuity equation,

$$(31)\quad V_{21} = \frac{W R T_{21}}{A_{21} P_{21}} = \frac{W R}{P_{21} A_{21}}\left(T_{T2} - \frac{V_{21}^2}{2 J c_p}\right)$$

Solving (31) for P_{21} and with (30),

$$(32)\quad P_{21} = \frac{W R}{A_{21} V_{21}}\left(\frac{W_T T_{TD} + W_N T_{TN}}{W} - \frac{V_{21}^2}{2 g J c_p}\right)$$

Combining (30) and (32),

$$(33)\left(\frac{W_N + W_T}{g} V_{21}\right) - \frac{W_N}{g} V_{IN} - \frac{W_T}{g} V_{IT} = A_{21} P^* - \frac{W R}{V_{21}}\left(\frac{W_T T_{TD} + W_N T_{TN}}{W} - \frac{V_{21}^2}{2 g J c_p}\right)$$

Multiplying (33) by V_{21} and expanding,

$$(34)\quad V_{21}^2\left(\frac{W_N + W_T}{g} - \frac{W R}{2 g J c_p}\right) - V_{21}\left(\frac{W_N V_{IN} + W_T V_{IT}}{g} + A_{21} P^*\right) + W R T = 0$$

Let:

$$(35)\quad B_1 = \frac{W}{g}\left(1 - \frac{R}{2 g J c_p}\right)$$

$$(36)\quad B_2 = -\left(\frac{W_N V_{IN} + W_T V_{IT}}{g} + P_1 A_2\right)$$

(37) $$B_3 = WRT_{T2}$$

Solving the quadratic (34) for velocity,

(38) $$V_{21} = -\frac{B_2}{2B_1} \pm \sqrt{\left(\frac{B_2}{2B_1}\right)^2 - \frac{B_3}{B_1}}$$

This equation yields both a subsonic and a supersonic solution; however, only the subsonic solution was pursued since the supersonic solution did not provide sufficient pressure recovery under the operating conditions investigated. With the known quantities,

(39) $$T_{21} = T_{T2} - \frac{V_{21}^2}{2gJc_p}$$

(40) $$P_{T2} = P_{21}\left(\frac{T_{T2}}{T_{21}}\right)^{\frac{\gamma-1}{\gamma}}$$

For the subsonic solution, the flow undergoes a compression process in the diffuser:

(41) $$\frac{W\sqrt{T_{21}}}{A_3 P_{21}}\sqrt{\frac{R}{g}} = \Phi = \sqrt{\frac{2\gamma}{\gamma-1}\left[\frac{T_{T2}}{T_{21}}\left(\frac{P_2}{P_{21}}\right)^{\frac{2}{n_c}} - \left(\frac{P_3}{P_{21}}\right)^{\frac{n_c+1}{n_c}}\right]}$$

This equation was solved by iteration to find P_3. If P_3 does not match P_{AMB} (atmospheric pressure) a new value for P_{IN} was assumed and the process repeated until P_3 matched P_{AMB}.

Having obtained P_3,

(42) $$T_3 = T_{21}\left(\frac{P_3}{P_{21}}\right)^{\frac{n_c-1}{n_c}}$$

(43) $$V_3 = \sqrt{2gJc_p(T_{T2} - T_{21})}$$

(44) $$P_{T3} = P_3\left(\frac{T_{T2}}{T_3}\right)^{\frac{\gamma}{\gamma-1}}$$

Test Results

The equations just described were used to predict exhauster performance utilizing a computer program. Since the primary purpose of the exhauster is to maintain a partial vacuum inside the hood, this was the major point of interest. A comparison of experimental and theoretical data is given in Figure 11. The discrepancy is due to the fact that the one-dimensional analysis ignores conditions from the inlet to the hood, assuming that the polytropic exponents are constant. This is not the case since secondary flow conditions are dependent on the varying polytropic process from the inlet to the hood. Table III shows the variation in polytropic exponents.

For the case where the secondary flow into the hood is a constant (i.e., turbine operation), the one-dimensional momentum analysis appears to provide a good approximation (Figure 11). It is to be noted that the experimentation was conducted with a nozzle total temperature about 20°F above the secondary flow total temperature. Increasing the nozzle total temperature will result in a very slight decrease in exhauster pumping capability, and for the allowable range of turbine operating temperatures, exhauster flow is virtually independent of total temperature.

5. Exhauster Design Evaluation

General

The most recent work on the design of ejectors available was published by Engle in 1963. [6] He presents a set of equations to be used to optimize the design geometry based on a one-dimensional analysis of incompressible flow. The present exhauster system meets the criteria set forth by Engle for driving-nozzle placement and secondary flow

entry. For optimum operation, the two streams should be parallel upon mixing tube entry to minimize losses. Secondary flow static pressure profiles (Figure 14) show a continuous decrease in static pressure up to the nozzle exit plane except at very high nozzle pressure ratios. The increase in static pressure at station 28 at high nozzle pressure ratios is probably due to separation.

At high secondary flow rates, the mixing tube static pressures show a fluctuation of 1.0 to 2.0 inches of mercury. However, the flow rate and hood total pressure remained steady in this regieme of operation. Since the secondary flow is choked at these pressure ratios, it was thought that the secondary flow rate might not be sufficient to stabilize the jet. This was not the case though for this system. The exhauster operation was very stable at high nozzle pressure ratios with no secondary flow. The instability only appears at high pressure ratios, without being felt inside the hood. The probable cause of the instability is the formation of a recirculation eddy due to separation effects along the mixing tube since the secondary flow is under an adverse pressure gradient.

Engle [10] also presents a method for determining the required area of the mixing tube. This is based on continuity, and is,

$$A = \frac{W}{\frac{V_{21}}{V_{IN}} V_{IN} \rho} \tag{45}$$

Substituting experimentally determined values into this equation for a nozzle pressure ratio of 2.22,

$$A = \frac{(8.011 + 3.91}{700(.441)(1.0564)} = .686 ft^2 \tag{46}$$

where ρ is an average density based on the average velocity computed at station five. The actual area of the mixing tube is .306 ft^2. Since Engle states that in practice the mixing tube area should be some 30 to 50 percent larger than the calculated value, the mixing tube area of this system is about 30% of the desired optimum.

Optimum mixing occurs according to Engle when the ratio between the velocity in the core and in the annulus is between .7 and .8 and that the length required is a function of the nozzle to secondary flow area. [6] In general, the optimum mixing length is between 7 and 10 diameters of the mixing tube. Removal of one section of the mixing tube left the exhauster operation virtually unchanged except at the higher pressure ratios. The velocity profiles taken at the diffuser entrance (Figure 5) for the short mixing tube indicate that the ratio between the core and annulus velocity increases with increasing nozzle pressure ratio, and falls short of the .7 to .8 desired velocity ratio which accounts for the reduction in pumping capability at the higher pressure ratios.

Optimum mixing tube length for this particular exhauster falls between the short and long tubes. However, as indicated from the exhauster performance, a wide variation in mixing tube length has little effect on system performance, since varying the length to diameter ratio from 5.46 to 10.9 had only a small effect on the operating characteristics.

It was not possible to duplicate turbine operating conditions as far as secondary flow rates and nozzle total pressure are concerned. However, extrapolating from experimental data, it should be possible to maintain a pressure ratio of about 5 to 1 for the converging-diverging

stator and a pressure ratio of about 6.3 to 1 for the converging turbine rotor stator for the transonic turbine. Exhauster operating conditions can be determined from Figures 11, 12, and 13.

Discussion

The basic hypothesis set forth by Yakovlevskii appears to be valid since the ejection property of a given nozzle is a function of its impulse, and empirical relations found for incompressible flow can be used to find a first approximation for the case of compressible flow. If the secondary flow rate or pressure is known, a one-dimensional momentum analysis can be used to determine operating conditions provided that the secondary flow is not choked. If the secondary flow is choked at the mixing chamber inlet, the method of Fabri can be used to predict operating characteristics. The method based on the hypothesis of Yakovlevskii has the advantage of producing a good approximation of the pumping characteristics with relative ease. However, the generality of the relationship between the secondary flow and nozzle impulse function was not tested for other ejector configurations.

Determination of the required length of mixing tube for a given ejector is still largely a matter of experience; however, it was shown that a wide variation in mixing length had very little effect on system operation. Mixing tube length to diameter ratios of from 7 to 10 should produce optimum operation. Calculation of the required mixing tube diameter based on the equation given by Engle indicates that the mixing tube diameter falls short of the desired optimum.

Although unstable conditions did appear in the mixing tube at high flow rates, the instability was not reflected in the hood total pressure. This fact coupled with the extrapolated performance figures

indicates that the exhauster will provide turbine operating pressure ratios in the design range.

Part II

Tests of a Reaction Turbine

1. Introduction

The second portion of the thesis describes a turbine test program carried out with the exhauster system to investigate the effects of high values of the isentropic head coefficient on turbine performance. The turbine tests were used also to correlate turbine performance with Reynolds number.

2. Turbine Installation

The turbine installation is identical to that described by Eckert except as noted here. [5] The turbine is an ARES MOD II instead of the Transonic Turbine. A cross section of the turbine is shown in Figure 15. Figures 16 to 18 show details of the rotor and stator construction. The instrumentation was modified by placing additional pressure taps in the shroud as shown in Figure 15. It is to be noted that the pressure tap locations have been projected into the one dimentional view while in actuality they are spaced around the periphery of the shroud. For this particular test program, the axial clearance was set at 0.41 inches while the radial clearance was set at 0.033 inches.

The cover plate flexure instrumentation mentioned by Eckert was installed to permit measurement of the torque and the axial force on the cover plate. [5]

3. Turbine Test Program

Flow Nozzle Calibration

The turbine flow nozzle installation and calibration techniques used are covered by Eckert. [4] Early calibration runs conducted by Eckert and Mr. L. T. Clark indicated that at low flow rates, the nozzle coefficient seemed to be a function of supply total pressure. Since this violates the principle of similarity, additional calibration runs

were made at supply total pressures of 20, 22, and 24 psia. Data was reduced using computer program FLOCAL with the exception that the expansion factor Y_1 for the nozzle was changed to that given by the ASME Power Test Codes. [5] Figure 19 shows the nozzle coefficient as a function of Reynolds number. The nozzle coefficient was based on vena contracta tap data since these have a lower tolerance. Examination of earlier calibration runs reveals a fairly large scatter (as much as ten percent) between vena contracta and flange tap data at low flow rates. For the calibration run shown in Figure 19, the difference between vena contracta and flange tap calculated flow rates is less than one percent. Therefore, a nozzle coefficient based on Figure 19 was used. An analytical expression for the flow nozzle coefficient as a function of Reynolds number was found by using the method of least squares to obtain a polynomial approximation. This was accomplished by a computer program yielding an eighth order polynomial for the best fit. The polynomial is,

$$C = -69.4248 + 65.42325x - 25.4166x^2 + 5.38697x^3 - 0.67816x^4 + 0.051422x^5 - 0.0022472x^6 + 0.000049356x^7 - 0.00000035959x^8 \quad (47)$$

where x = Reynolds number multiplied by 10^{-5}. The maximum deviation in the flow range of interest (1.6 to 4.5 lbm/sec) occurs at a Reynolds number of 6×10^5 and is .003. The polynomial is only valid for Reynolds numbers in the range of 4 to 12 times 10^5.

Turbine Flow Rate Determination

The turbine flow rate is equal to the total rate measured by the nozzle less the plenum labyrinth leak rates. Total nozzle flow was determined by means of the ASME standard equations using an initial

nozzle coefficient of 1.03. [15] Vena contracta tap data was used throughout, with differential pressure measured on a 96 inch water manometer, and flow nozzle static pressure measured on a 96 inch mercury manometer. Then, after calculating the Reynolds number, the flow nozzle coefficient was corrected by application of the eighth order polynomial described above and a new flow rate determined.

Calculation of the plenum labyrinth leakage flow rates utilized the expressions given by Eckert which were determined from experimental data. [4]

Turbine Tests

The turbine was rotated on 14 November 1966 with the bottom portion of the hood installed to check the instrumentation. The shaft seal labyrinth was bored out to 1.258 inches diameter to accommodate a new quill shaft without recutting the chambers for a seal tooth clearance of 0.040 inches. The turbine was run up to about 13,000 RPM. Upon shutting down, it was noticed that the quill shaft had rubbed on the labyrinth, scoring the shaft. The shaft was buffed and reinstalled with the labyrinth realigned. When the turbine was rotated again on 16 November, shaft rubbing occurred at about 7,000 RPM. The shaft was measured and found to be 0.005 inches out of round. It was then turned down 0.005 inches and the labyrinth enlarged so that after alignment the clearance was 0.030 inches radially at the dynamometer end and 0.015 inches radially at the hood end. This prevented further rubbing when the turbine was rotated on 18 November 1966 with the full hood and exhauster installed. The present labyrinth is only a temporary device and will be replaced. Since the only result of the increased leakage into the hood is the degradation of the system's capability to maintain

a partial vacuum inside the hood, the existing labyrinth is suitable for continued testing until a replacement is obtained. The purpose of the first run was to investigate the performance limits of the system. With the ARES MOD II turbine installed, a pressure ratio of 1.79 was attained. Since the turbine efficiency is much greater than that of the exhauster, a reduction in turbine flow rate with the corresponding increase in exhauster flow rate resulted in a decrease in pressure ratio. The exhauster is capable of maintaining a partial vacuum of one-half an atmosphere in the hood with a turbine flow rate of 3.88 lbm/sec. Since this particular turbine has been the subject of an extensive test program without the hood installed reaching a maximum pressure ratio of 1.55, it was decided to run at pressure ratios of 1.3, 1.4, 1.5, 1.55, and 1.65 with values of the isentropic head coefficient varying between the design value of 2.609and 4.5.

Turbine testing was started on 22 November 1966. During the run, the RPM readout was checked by means of a strobotac and it was found that the RPM read out was faulty. The system was checked thoroughly, and the difficulty finally corrected by replacing the leads between the counter and the flux cutter at the turbine. The final test was conducted on 23 November 1966, when testing was halted due to time considerations. Under the present test rig set-up, the flux cutter and pickup is located inside the hood. It is felt that it would be advantageous to move the unit outside the hood where it would be readily accessible for adjustment.

Data Reduction and Results

The turbine flow rate was determined as described in the previous section. Total inlet temperature was determined from a probe installed

in the 6 inch pipe of the stator assembly. Inlet total pressure was taken from the average of the six Kiel probes (Figure 15) placed radially at the stator inlet. The hood pressure taken from the average of the eight hood static pressure taps was used for the turbine discharge static pressure. The turbine speed and dynamometer moment complete the quantities required to determine turbine performance. Data was reduced using the method of Vavra by a computer program. The method of analysis is being published in a Thesis by Lt. M. W. Wallace, U.S. Naval Postgraduate School, Monterey, California. [13]

The following referred values were obtained from the performance analysis;

for $\gamma = c_p/c_v = 1.4$:

(49) $\Theta = T_{To}/518.4$

(50) $\delta = P_{To}/14.7$

(51) $M_{ref} = \frac{M_B}{\delta}$ = referred moment (Ft-lb)

(52) $N_{ref} = \frac{N_R}{\delta}$ = referred turbine speed (RPM)

(53) $\dot{W}_{ref} = \frac{\dot{W}\sqrt{\Theta}}{\delta}$ = referred flow rate (lbm/sec)

(54) $HP_{ref} = \frac{HP}{\sqrt{\Theta}\,\delta}$ = referred horsepower (HP)

(55) $K_{is} = \frac{\Delta h_{is}}{U_1^2/2}$ = head coefficient

The turbine efficiency is a total to static efficiency, defined by

(56) $$\eta = \frac{\frac{HP}{\delta\sqrt{\Theta}}}{\frac{HP_{TH}}{\delta\sqrt{\Theta}}}$$

where HP_{th} is the theoretical horsepower based on an isentropic expansion from the inlet total temperature to the static pressure in the hood, or,

$$(57) \qquad \frac{HP_{tn}}{\delta\sqrt{\Theta}} = \left(\frac{\dot{W}\sqrt{\Theta}}{\delta}\right)\left[1 - \left(\frac{P_2}{P_{TO}}\right)^{\frac{\gamma-1}{\gamma}}\right]\frac{70.3987}{(\gamma-1)}$$

where

P_2 = discharge pressure (lb/ft^2)

P_{TO} = inlet total pressure (lb/ft^2)

Determination of turbine Reynolds numbers is rather arbitrary as to choice of characteristic lengths and velocities. After a perusal of the literature on the subject of Reynolds number effects in turbomachines, two sets of quantities were chosen, one based on rotor tip speed, and one based on the flow rate and mean radius. They are defined as,

$$(58) \qquad RE = \frac{\dot{W}}{\mu r_m}$$

and

$$(59) \qquad RT = \frac{2\pi RPM\,\rho R}{720\,\mu}$$

where

$\dot{W}$ = weight rate of flow (slugs/sec)

μ = viscosity at turbine inlet total conditions ($lb.sec/ft^2$)

ρ = density at inlet total conditions ($slugs/ft^3$)

R = rotor radius (inches)

r_m = mean rotor radius (ft)

The referred values of horsepower, moment, and flow rates are shown in Figures 20 through 22. Turbine efficiency plotted as a function of the isentropic head coefficient is shown in Figures 23 and 24. Although great care was used in attempting to keep the pressure ratio at the set value, the wide number of system variables caused minor deviations from the ratio. Table IV gives the actual pressure ratio at each data point

and the maximum deviation.

4. Discussion of Results

General

The exhauster system functioned well, maintaining a hood pressure of about one half of the atmospheric pressure. At a pressure ratio of 1.65 with a turbine flow rate of 3.88 lbm/sec a bothersome low frequency instability was noted in the hood pressure which was reflected in turbine operation. This fluctuation resulted in a low frequency flow rate fluctuation of as much as two inches of water in differential pressure across the flow nozzle and an RPM variation on the order of 150. All of the turbine pressure readings were made on one manometer bank by using a Polaroid camera to photograph the board, and since the flow rate differential pressure, turbine RPM and dynamometer reading were taken as quickly as possible, the fluctuation did not seem to induce undue scatter in the data.

The torque capsules are calibrated prior to each run by applying known weights to a lever arm. For dynamometer calibration, the torque capsule must be removed from the unit and placed in a special stand. The present calibration technique involves jiggling or tapping the capsule as the weights are varied through several cycles until the readout produces consistent values. For the last run, the stator axial force capsule could not be calibrated at all, but since data reduction by the method used does not require this value, no attempt was made to correct this difficulty. It is felt that the present method of calibrating the torque capsules mechanically is unsatisfactory both from the standpoint of accuracy and time. Calibration of the torque capsules required as much as three hours, severely limiting the amount of

experimentation that could be accomplished during the normal working day. Provided that the capsules are not disturbed, electrical calibration would be both rapid and accurate. The present axial force measurements when used in a momentum analysis do not produce results consistent with those obtained from continuity, and the difficulty almost certainly lies with the axial force measurements.

The turbine is designed for an isentropic head coefficient of 2.609 at a pressure ratio of 1.5. Neither increasing the pressure ratio nor increasing the isentropic head coefficient did result in an increase in efficiency (Figures 23 and 24). At pressure ratios of 1.3 and 1.65 a dip in efficiency was noted with increasing head coefficients that is not present at the other pressure ratios. The reason for this dip is unknown, and it does not match the theoretical data given by Vavra.[11] It is to be noted that this particular turbine is capable of operating under off-design conditions with very little reduction in efficiency.

Although a great deal of research has been devoted to investigating Reynolds number effects in turbomachines, the results are still inconclusive. Figure 25 shows the Reynolds number based on flow rate plotted versus turbine efficiency for three runs. Run 50 was conducted by the author using the full hood and exhauster installation. Runs 40 and 45 were conducted by Professor M.H. Vavra with the turbine discharging to the atmosphere at pressure ratios of 1.3, 1.4, and 1.5. Run 45 used the same axial clearance of 0.41 inches and tip clearance of 0.033 inches that were used on Run 50, whereas for Run 40, at an axial clearance of 0.410 inches the tip clearance was set to 0.015 inches. For the plotting of the data, the efficiency at each pressure ratio was averaged and plotted as a single point since the Reynolds number variation at a

given pressure ratio is insignificant. Reynolds number based on rotor tip speed is shown plotted versus turbine efficiency in Figure 26.

NASA investigators on a number of turbines using the flow rate definition of Reynolds number found that turbines operating with Reynolds numbers above 2×10^5 showed no variation in loss parameters with Reynolds numbers. [8] They also found that different turbines operating in the same range of Reynolds numbers had different loss parameters. This seems to point out that either the losses in turbines operated above a Reynolds number of 2×10^5 are not a function of Reynolds number or that the machine characteristics used to determine the Reynolds number are not correct.

Examination of Figure 26 which uses the Reynolds number based on rotor tip speed fails to show any trend, and again it appears that the efficiency is not a function of the Reynolds number within the range of investigation.

Losses in turbomachines are due to viscous effects and since Reynolds number is a measure of these effects, it would seem only natural that some correlation should exist between Reynolds number and turbine efficiency. The primary difficulty lies in the elusiveness of the actual loss mechanisms associated with the flow in turbomachinery, and therefore, the inability of the investigator to be capable of relating the loss parameter to Reynolds number. A more detailed study would involve various definitions of characteristics lengths and velocities over a wide range of Reynolds numbers. This is a difficult task experimentally when dealing with a compressible fluid due to the wide range of temperatures and pressures required to obtain a significant variation in Reynolds number.

5. Conclusions and Recommendations

The ARES MOD II turbine appears to reach its maximum efficiency at the design pressure ratio and the design value of the isentropic head coefficient. However, it is capable of operation over a wide range of pressure ratios and isentropic head coefficients with only a slight reduction in efficiency. For the operating ranges tested, turbine performance does not seem to be related to Reynolds number.

The weakest point of the present turbine test rig is the torque capsule calibration. A suitable means of electrical calibration should provide both speed and accuracy in calibration. The axial force measurements, both on the stator and coverplate, seem to be in error, due to some unknown cause. Therefore, it is recommended that the present instrumentation be improved, possibly by installing some type of hydraulic measuring device.

BIBLIOGRAPHY

1. Abramovich, G. N., The Theory of Turbulent Jets, translation by Scripta Technica, MIT Press, Cambridge, Massachusetts, 1963.

2. Addy, A. L. and Chow, W. L., On the Starting Characteristics of Supersonic Ejector Systems, ASME Transactions, Journal of Basic Engineering, Vol. 86, series D , Number 4, December, 1964.

3. Alexander, Baron, and Commings, Transport of Momentum, Mass and Heat in Turbulent Jets, U. of Illinois Engineering Experiment Station, Bulletin Series No. 413, Vol. 50, Number 66, May, 1953.

4. Eckert, R. H., Determination of Flow Rates Transonic Turbine Test Rig, TN 66T-1, U.S. Naval Postgraduate School, Monterey, California, January, 1966.

5. Eckert, R. H., Performance Analysis and Initial Tests of a Transonic Turbine Test Rig, Thesis, U.S. Naval Postgraduate School, Monterey, California, May, 1966.

6. Engle, M. O., Some problems in the Design and Operation of Jet Ejectors, Proceedings of the Institution of Mechanical Engineers Steam Plant Group. Thermodynamics and Fluids Group, Vol. 177, No. 133, 1963, London, England, p. 350.

7. Fabri, J. and Paulson, J., Theory and Experiments on Supersonic Air-to-Air Ejectors, NACA TM 1410, September, 1958.

8. Holski, D. E. and Stewart, W. L., Study of NASA and NACA Single-Stage Axial Flow Turbine Performance as Related to Reynolds Number and Geometry, Transactions of the ASME, Journal of Engineering for Power, Vol. 86, Series A, Number 3, July 1964, pp. 296-298.

9. Vavra, M. H., Problems of Fluid Mechanics in Radial Turbomachines (Rhode-Saint-Genese, Belgium, Von Karman Institute for Fluid Dynamics, 1965) VKI Course Note 55a, pp. 22-35.

10. Vavra, M. H., Theoretical Evaluation of Exhauster System of Transonic Turbine Test Rig, TN65T, U.S. Naval Postgraduate School, August, 1965.

11. Vavra, M. H., Aero-Thermodynamics and Flow in Turbomachines, John Wiley and Sons, New York, New York, 1960.

12. Viktorin, K., Investigation of Turbulent Mixing Processes, NACA TM 10 96, 1946.

13. Wallace, M. W., Performance Analysis of Two Reaction Turbines Thesis, U.S. Naval Postgraduate School, Monterey, California. To be published in December, 1966.

BIBLIOGRAPHY
(continued)

14. Yakovlevskii, O. V., Hypothesis on Universal Ejection Properties of Turbulent Jets of Gas, and Its Application, Translated from Izvestiga Akademii Navk SSK, Otdelenie Technicheskikh Navk, Mexanka, e Mashinostroenie, No 3, 40-54 (1961) by Ingeborg V. Baker, Translation Branch, Redstone Scientific Center Information Center, RSlc-108, 20 December 1963, p. 5.

15. Flow Measurement, Chap. 4, Part 5, Supplement to ASME Power Test Codes, ASME, New York, New York, 1959, p. 74.

Table I

$\frac{G}{G_o}$ as a function of $P_{T\,NOZZLE} / P_{AMB}$

$\frac{G}{G_o}$	$P_{T\,NOZZLE} / P_{AMB}$
1.481	1.75^{+}
1.482	1.88^{+}
1.482	2.10^{+}
1.478	2.16^{+}
1.468	2.36^{+}
1.482	1.78^{++}
1.480	2.10^{++}
1.480	2.22^{++}
1.470	2.50^{++}
1.421	1.14^{+++}
1.468	1.29^{+++}
1.482	1.41^{+++}

\+ Long Mixing Tube
++ Short Mixing Tube
+++ Subsonic Nozzle Operating Region

Table II

Centerline Velocities, ft/sec, $P_{T_N}/P_{AMB} = 2.22$

Station	Theoretical	Experimental
1	1400	1100+
2	1270	1260
3	920	960
4	735	760
6	570	650++

+ Station 1 is the station where the centerline total pressure is much lower than the off-center total pressure, and the experimental value is in question.

++ Station 6 is located sufficiently far downstream of the point where the mixing process is complete and the flow is that of turbulent flow in a pipe and is not expected to conform to the power law assumed for the centerline velocity.

Table III

Φ and $\Phi_{critical}$ as a Function of Secondary Mass Flow Rate

Process from Secondary Flow Inlet to Annulus

Φ	$\Phi_{critical}$	W(lbm/sec)	n
.2614	.2667	3.43	1.056
.2755	.2759	3.62	1.060
.2876	.2891	3.785	1.066
.2986	.3119	3.93	1.0770
.3046	.3348	4.00	1.089

Process from Hood to Annulus

Φ	$\Phi_{critical}$	W(lbm/sec)	n
.3509	.5950	3.43	1.295
.3952	.5874	3.62	1.287
.4475	.6015	3.78	1.302
.5150	.6034	3.93	1.304
.5616	.6125	4.00	1.3140

FIG 2

TRAVERSING PROBES

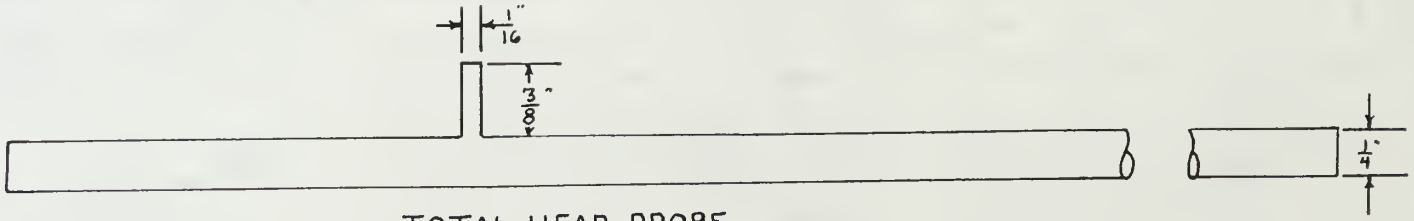

TOTAL HEAD PROBE

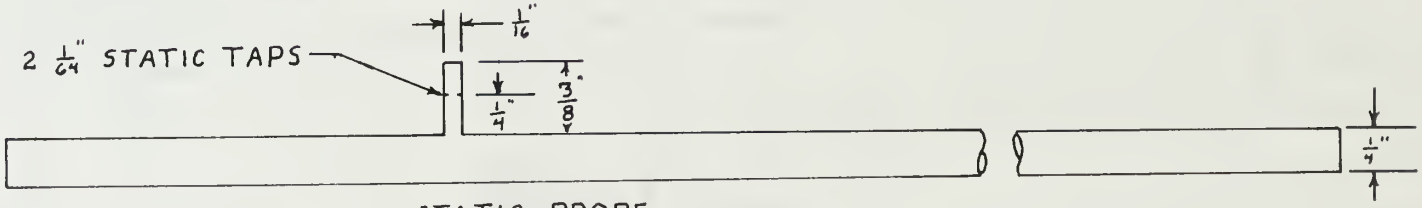

STATIC PROBE

NOT TO SCALE

FIG 3

VELOCITY PROFILE STATION

$\frac{P_{T\,NOZZLE}}{P_{AMB}} = 2.24$

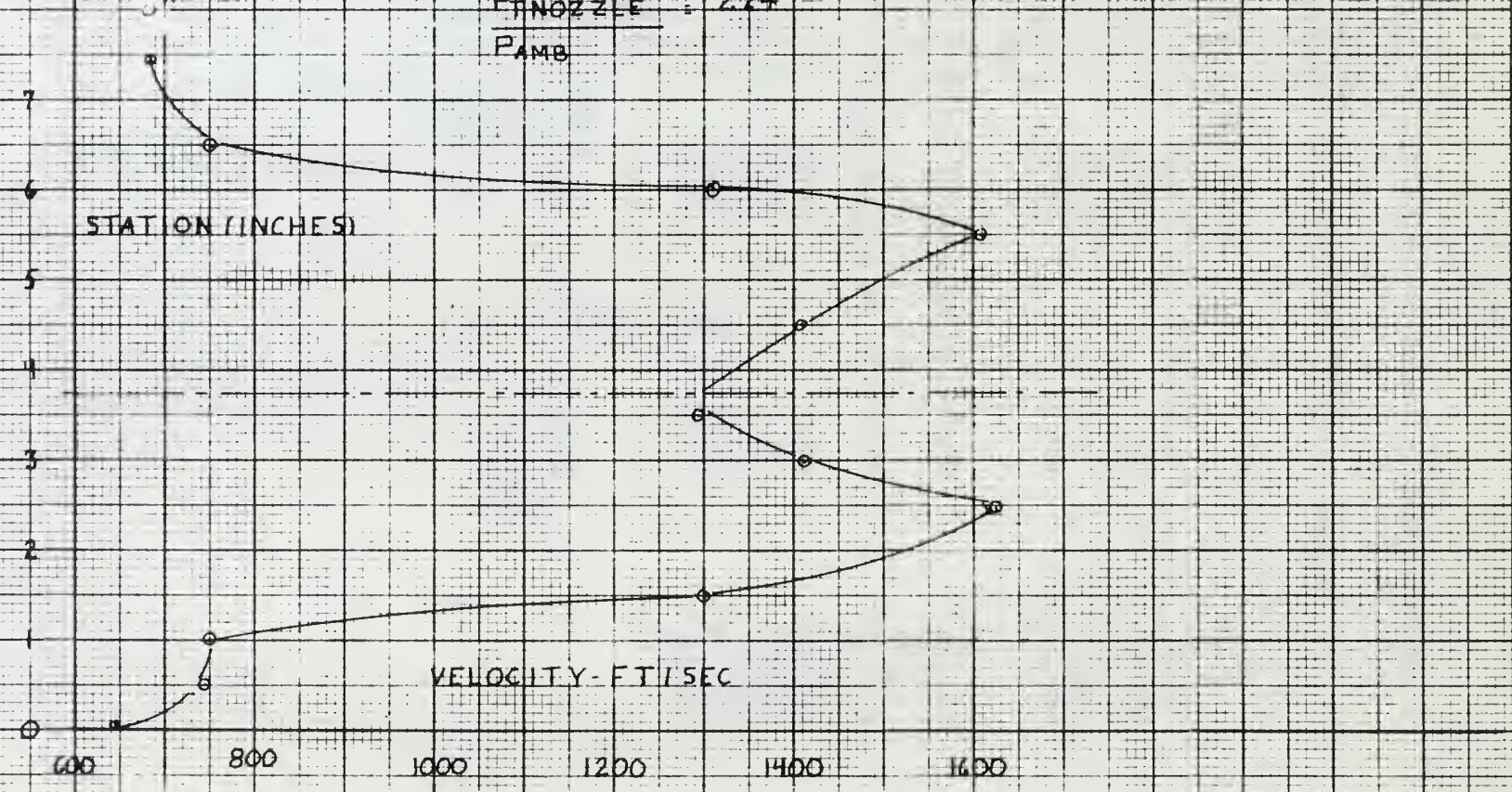

FIG 4

VELOCITY PROFILES - LONG MIXING TUBE

$\frac{P_{TNOZZLE}}{P_{AMB}} = 2.22$

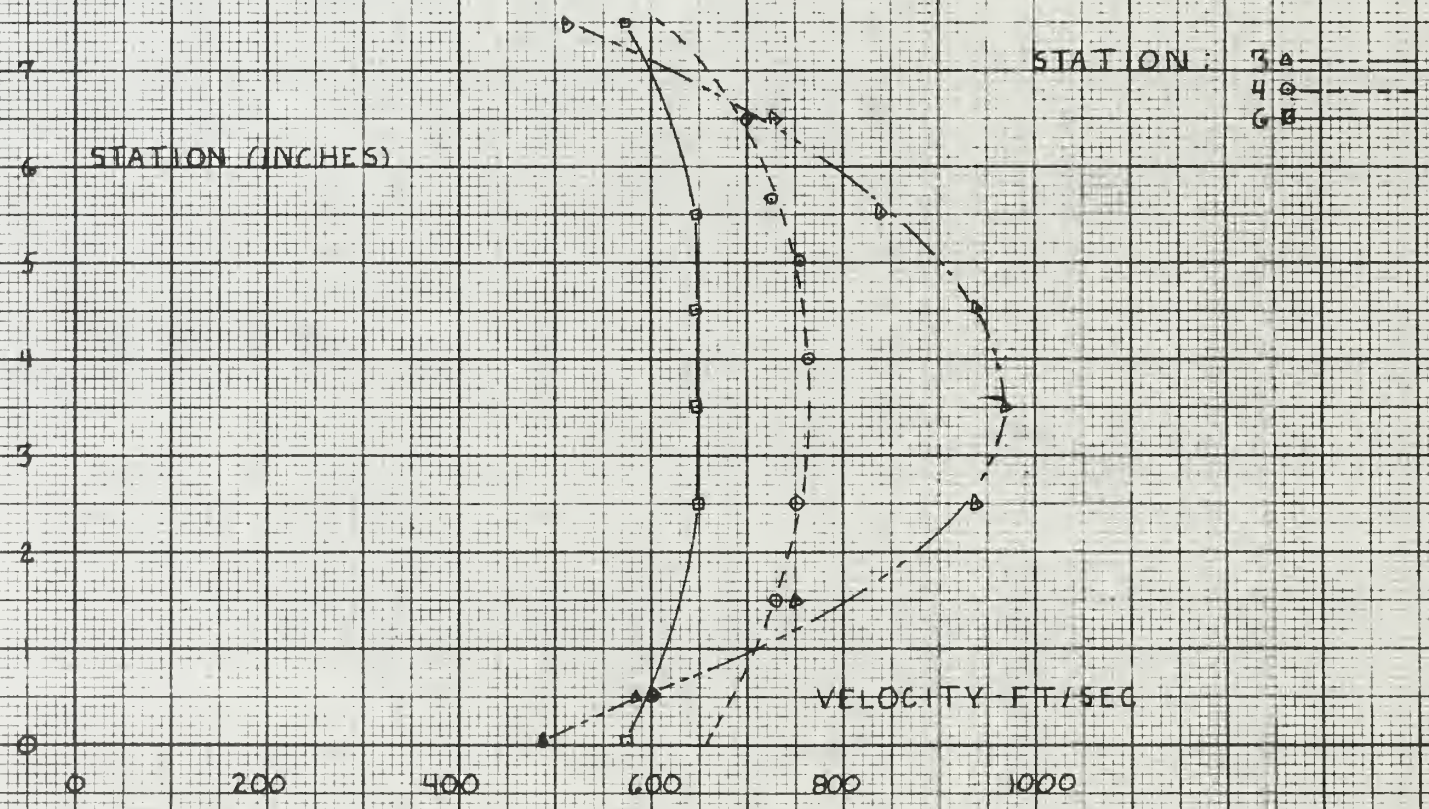

FIG 5

VELOCITY PROFILES - DIFFUSER ENTRANCE

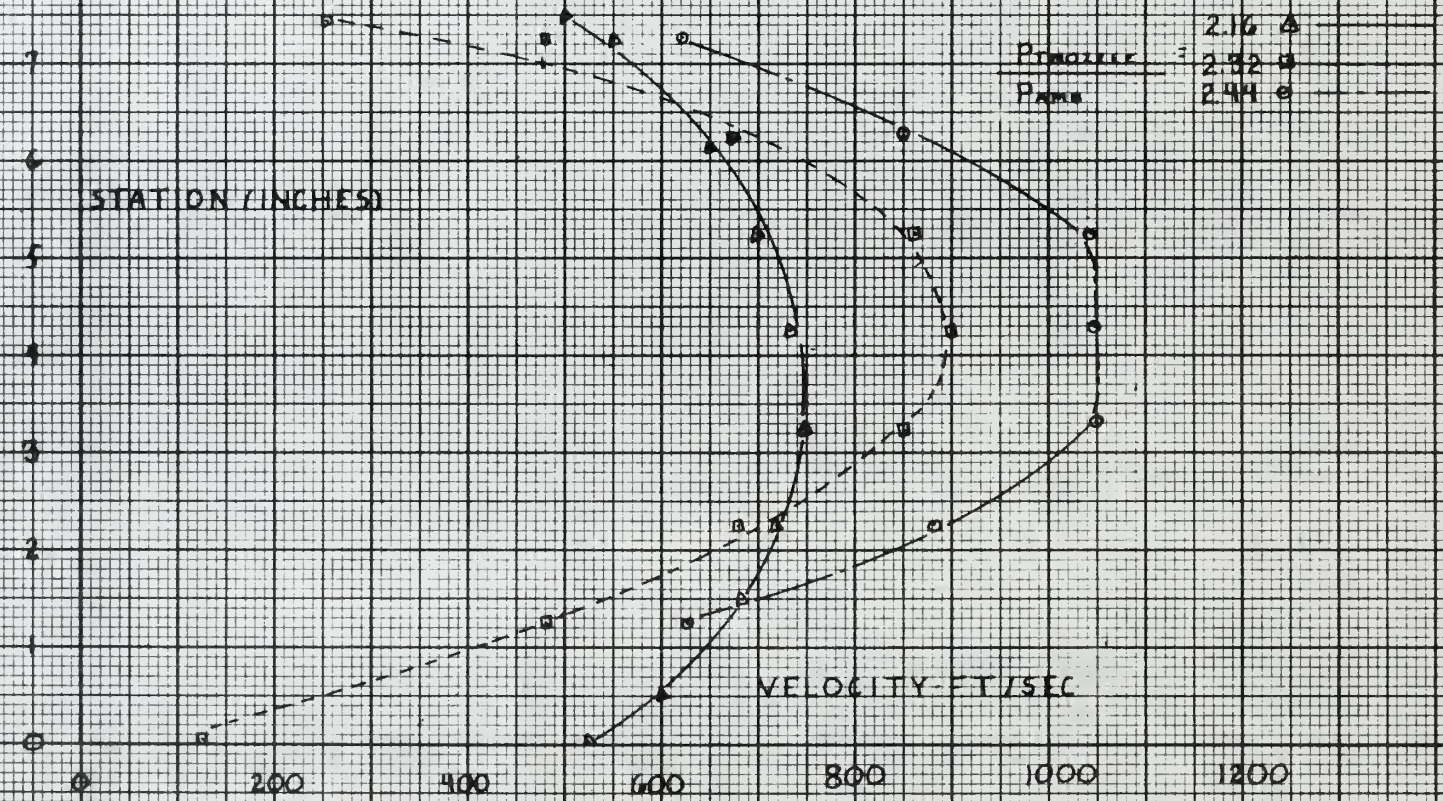

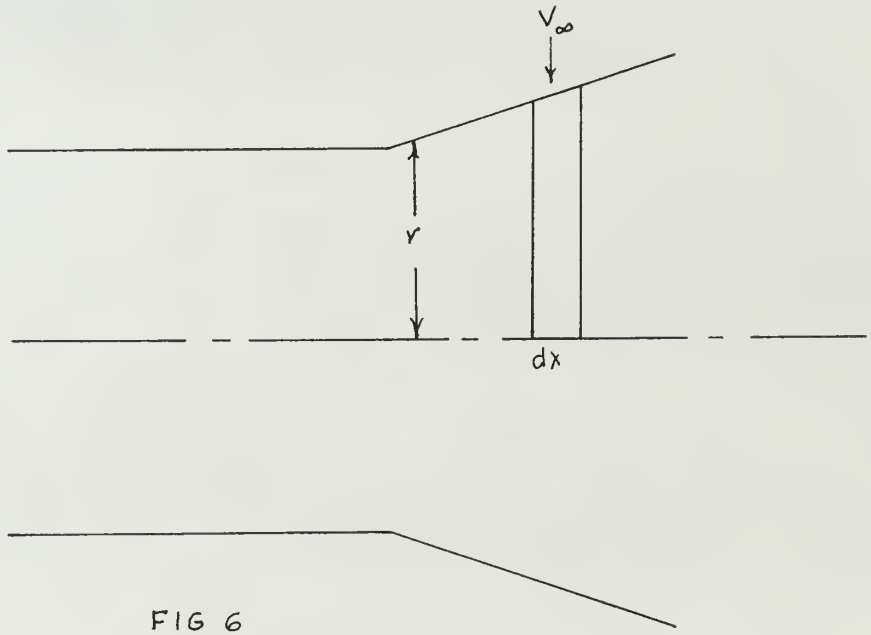

FIG 6
AXISYMMETRIC JET

FIG 7

IMPULS FUNCTION VERSUS $\sqrt{\frac{g}{d_c}}$

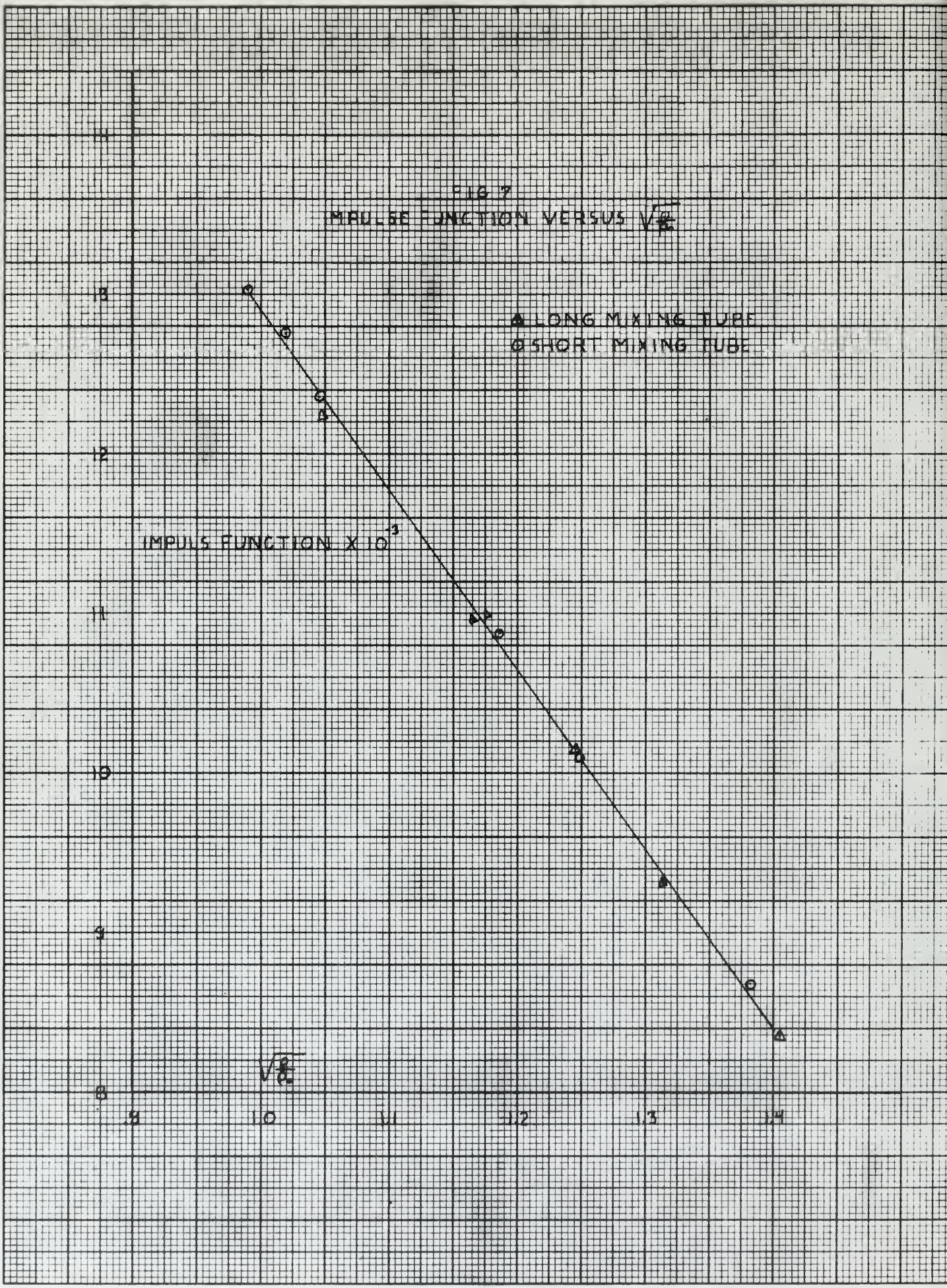

FIG 8

IMPULSE FUNCTION VERSUS SECONDARY FLOW RATE

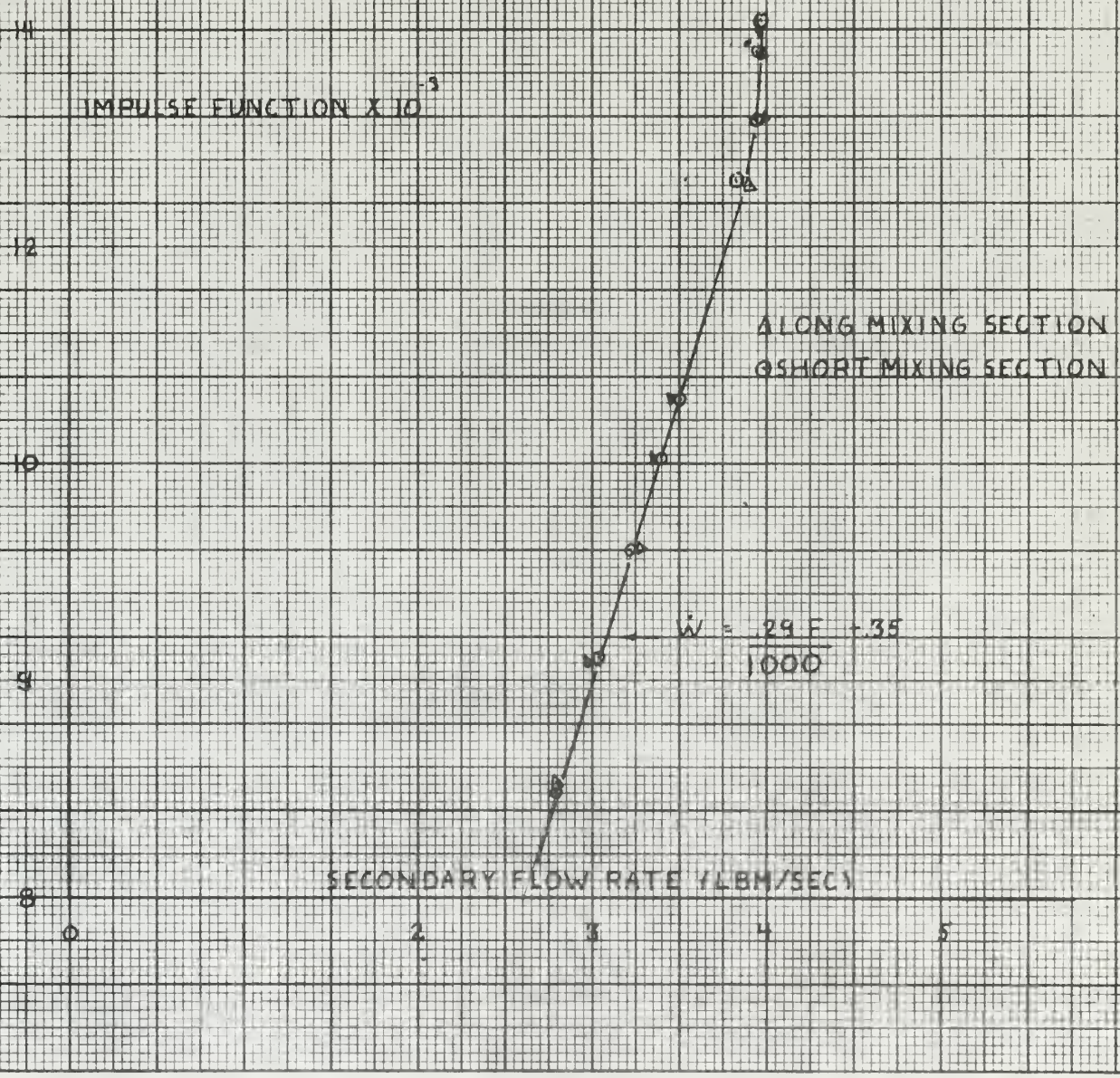

FIG 8

MIXING TUBE STATIC PRESSURE GRADIENT

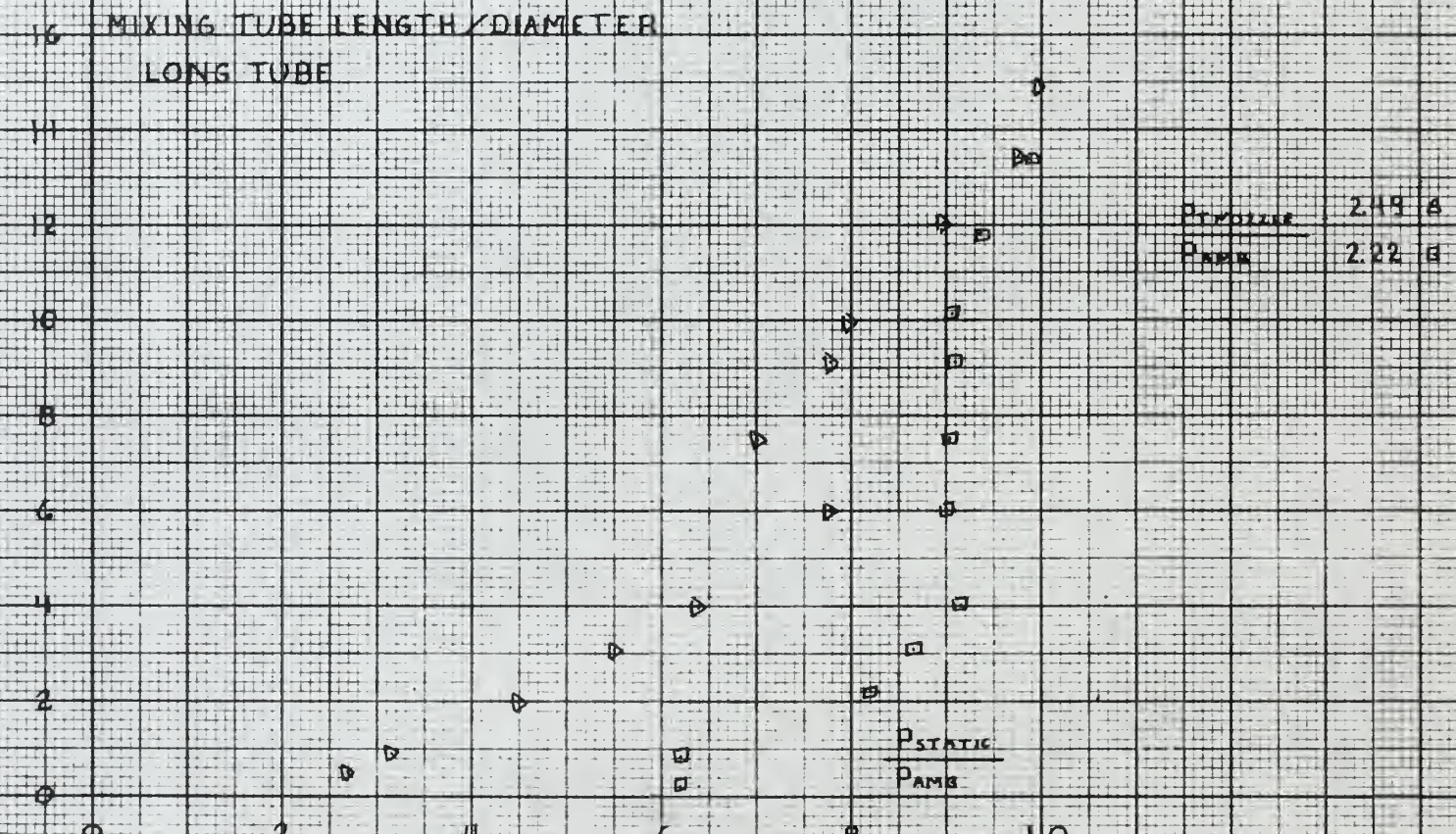

FIG 10
MIXING TUBE STATIC PRESSURE GRADIENT

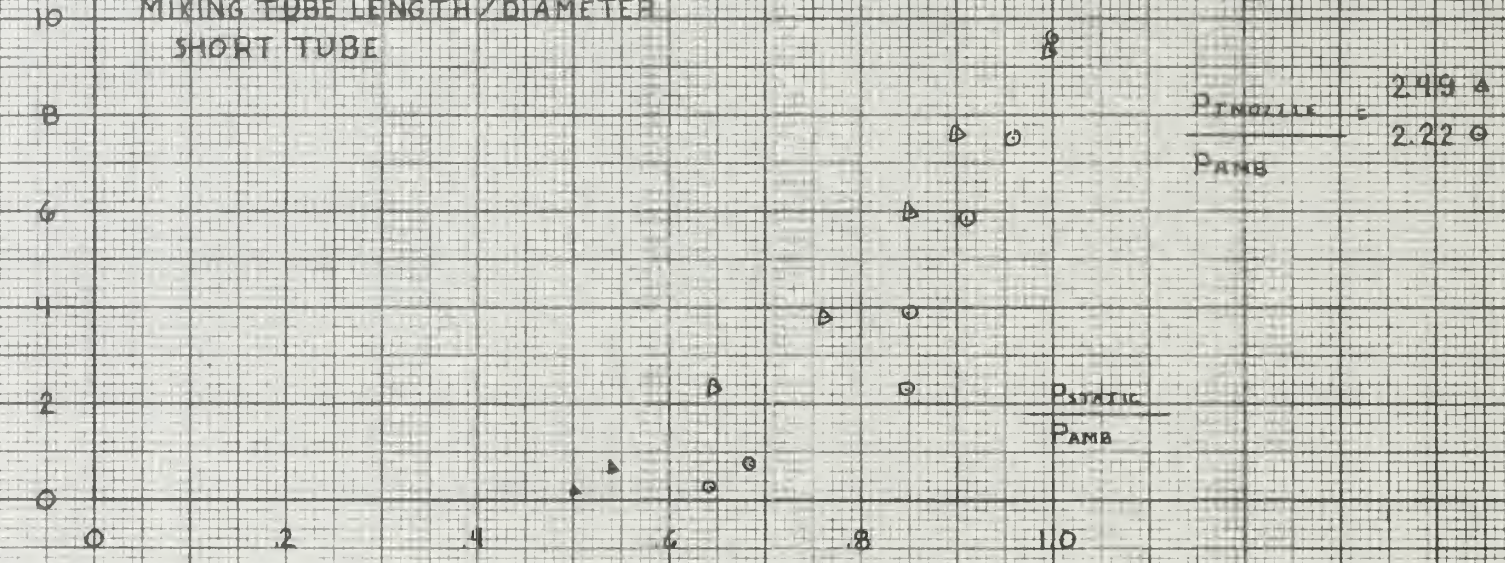

FIG 11

EXHAUSTER PERFORMANCE

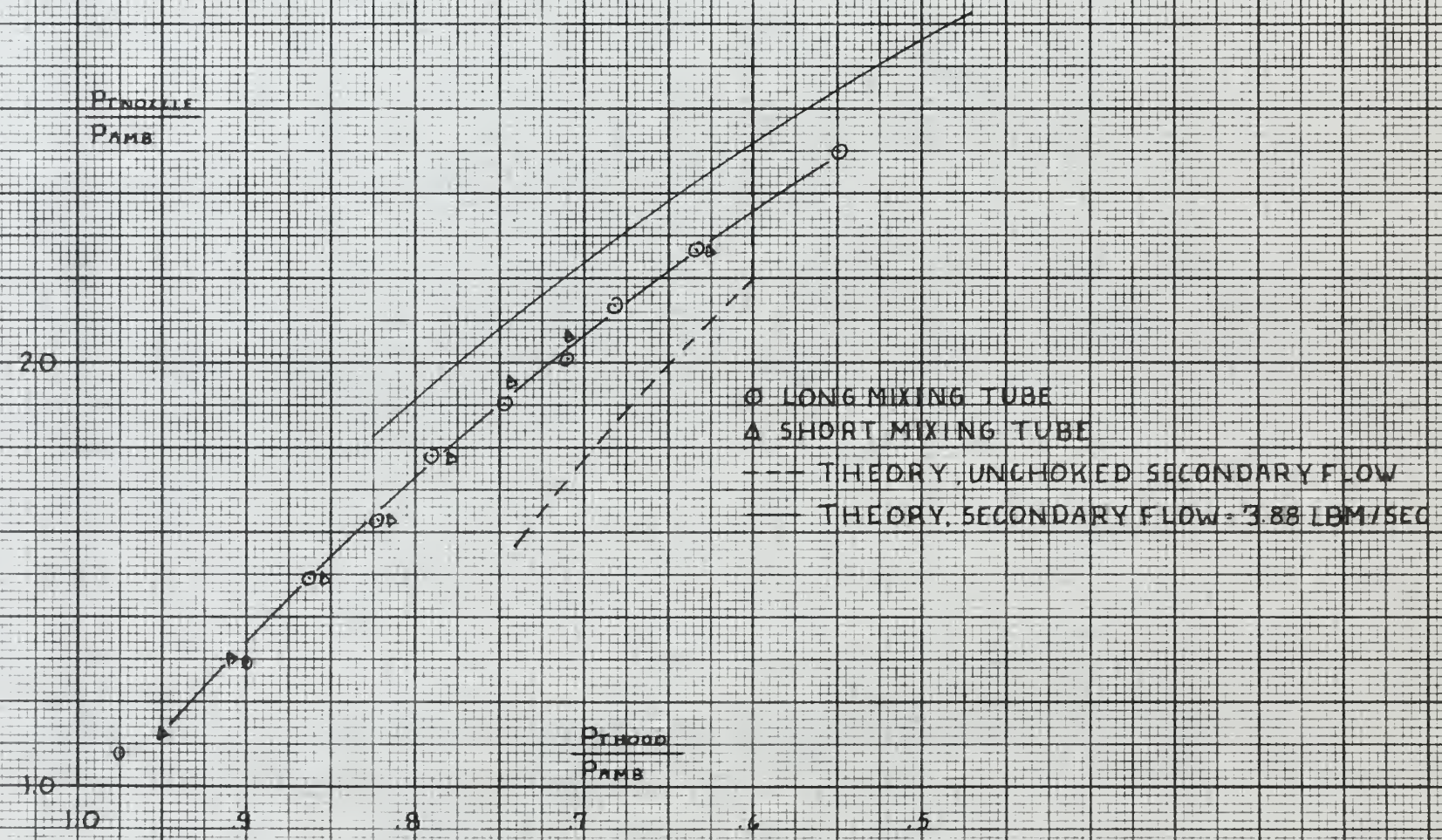

FIG 12

SECONDARY FLOW RATE VERSUS DRIVING NOZZLE PRESSURE RATIO

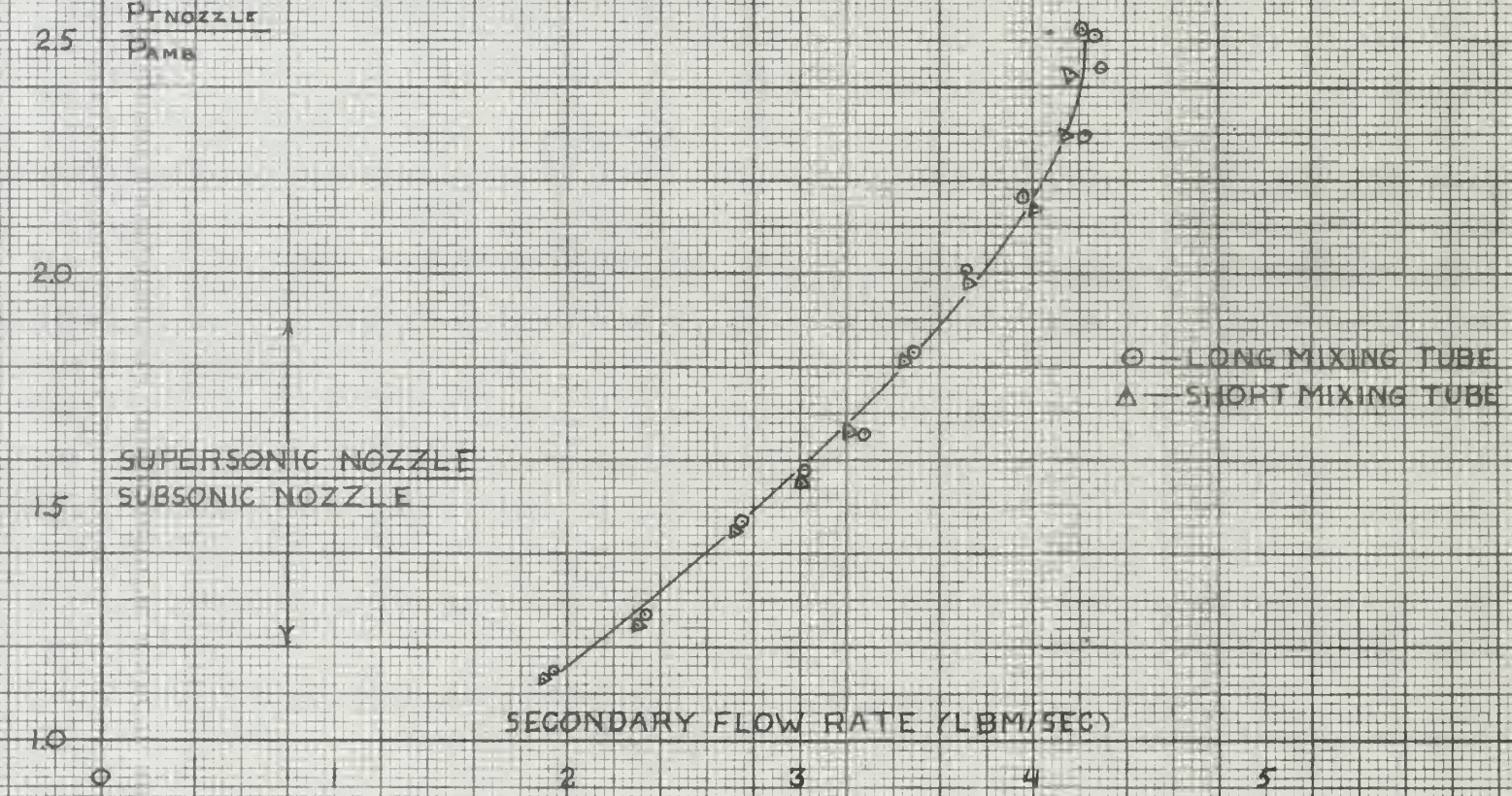

FIG 13

HOOD PRESSURE RATIO VERSUS SECONDARY FLOW RATE

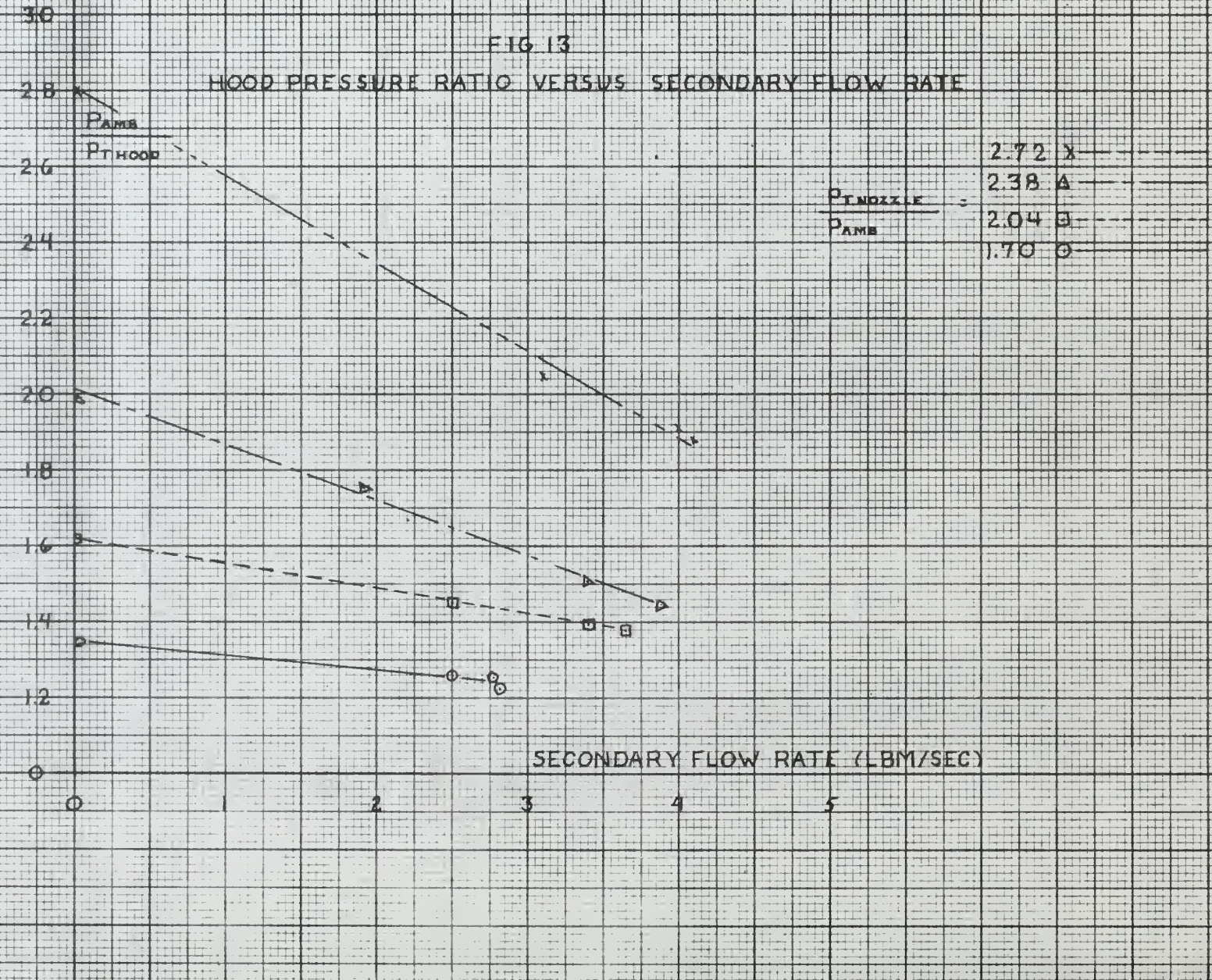

FIG 14

ENTRY SECTION STATIC PRESSURE PROFILES

LONG MIXING TUBE

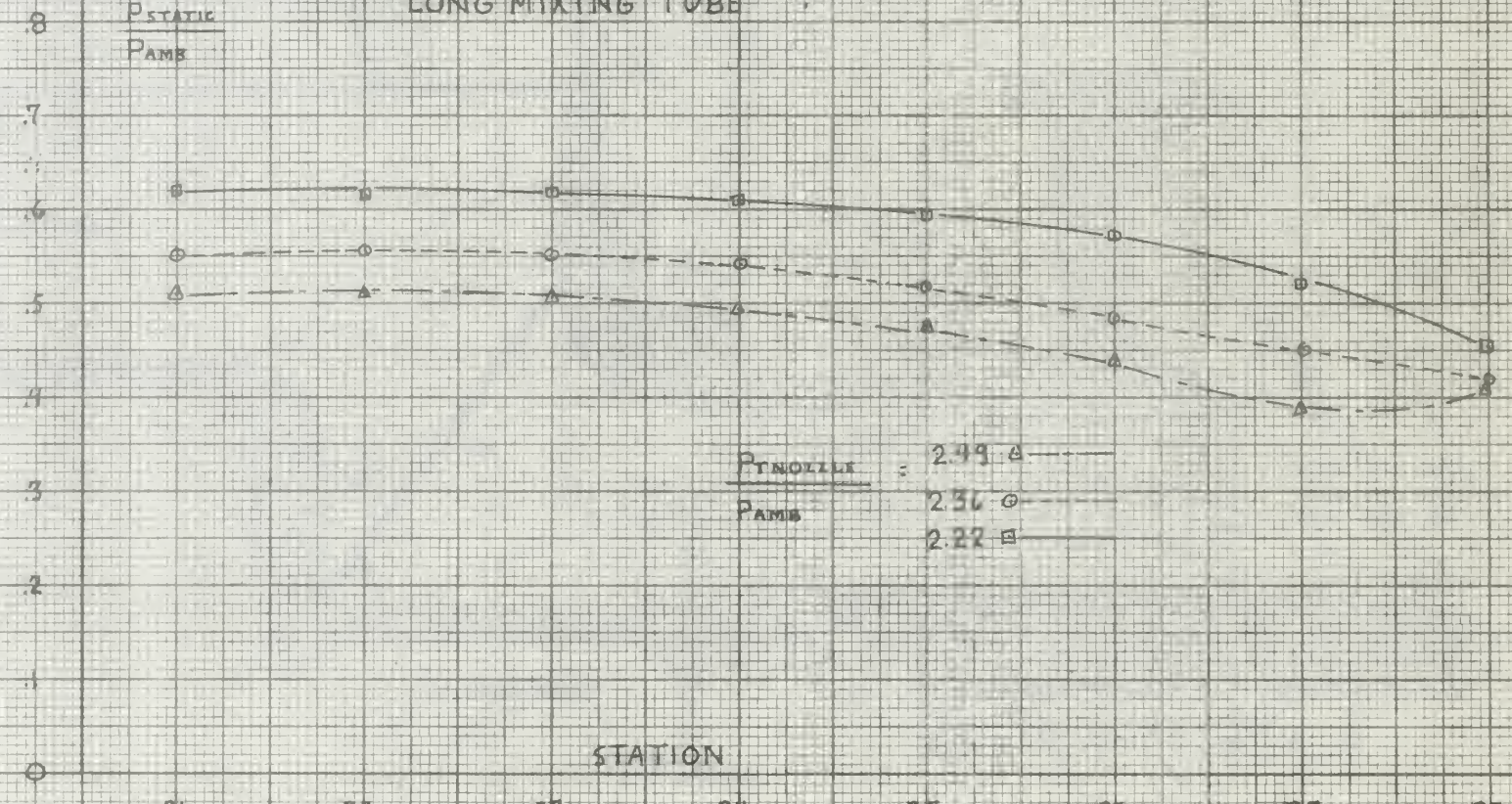

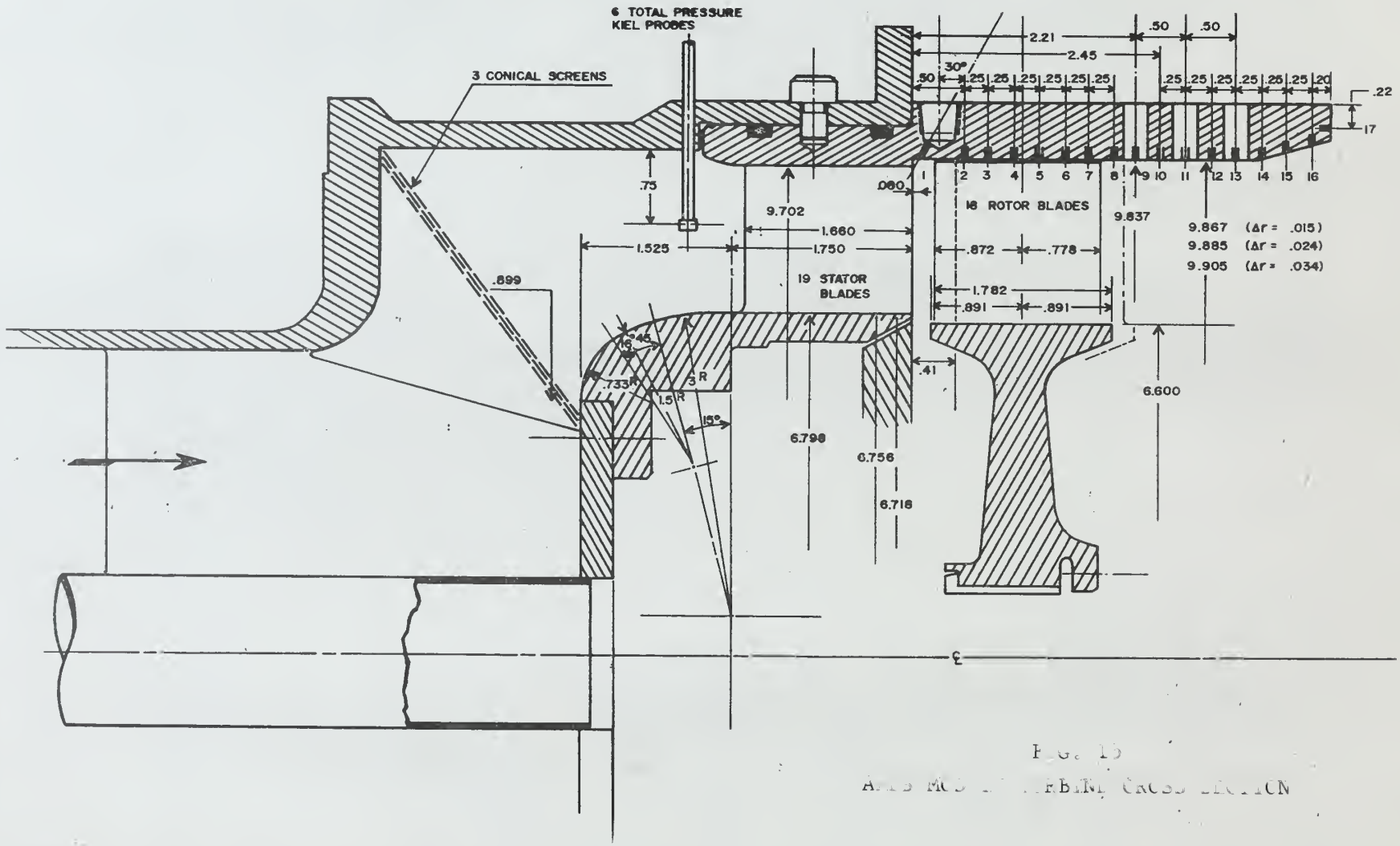

Fig. 15

AMES MOD 1 TURBINE CROSS SECTION

FIG. 16
TURBINE STATOR BLADE PROFILE

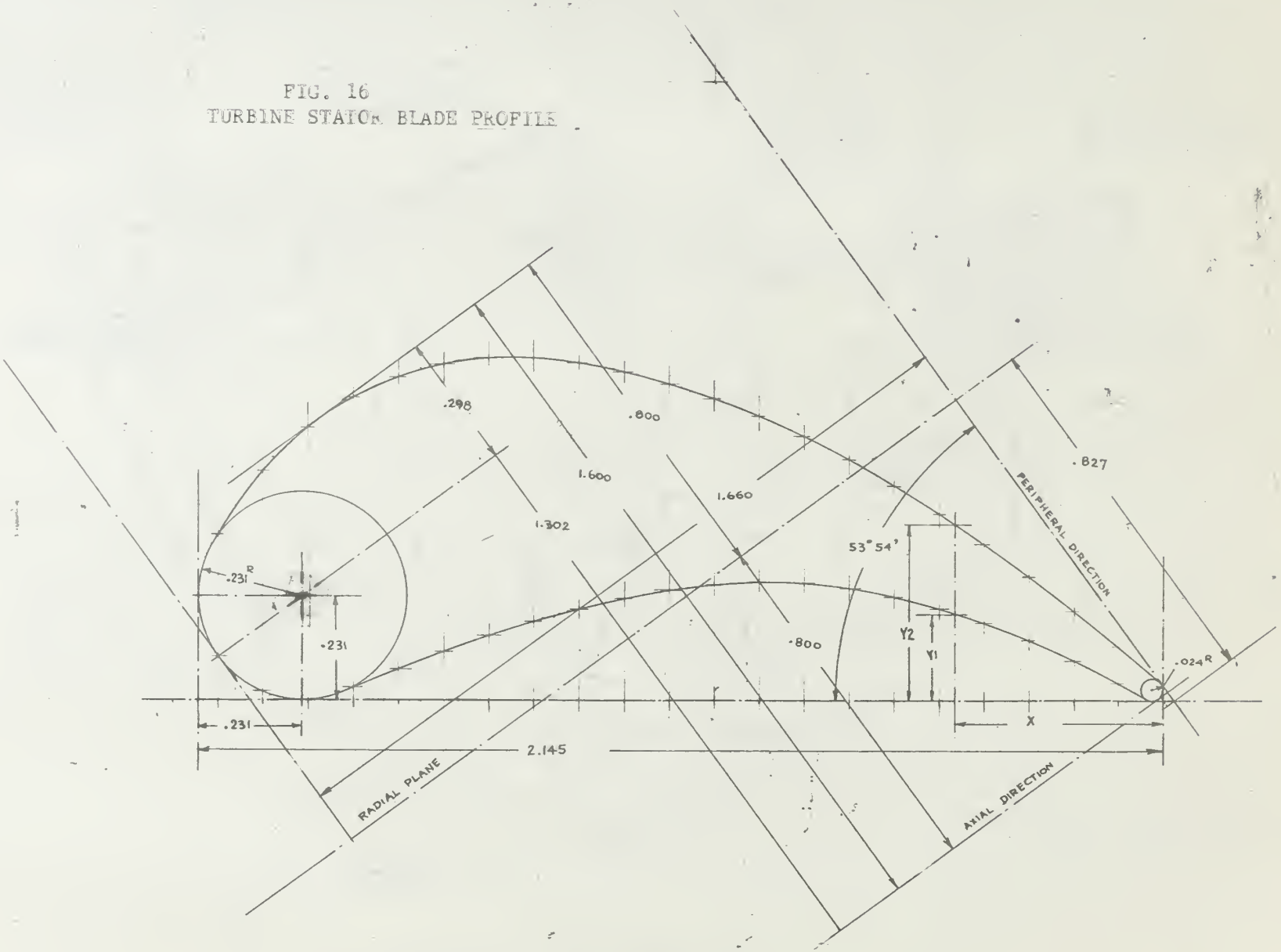

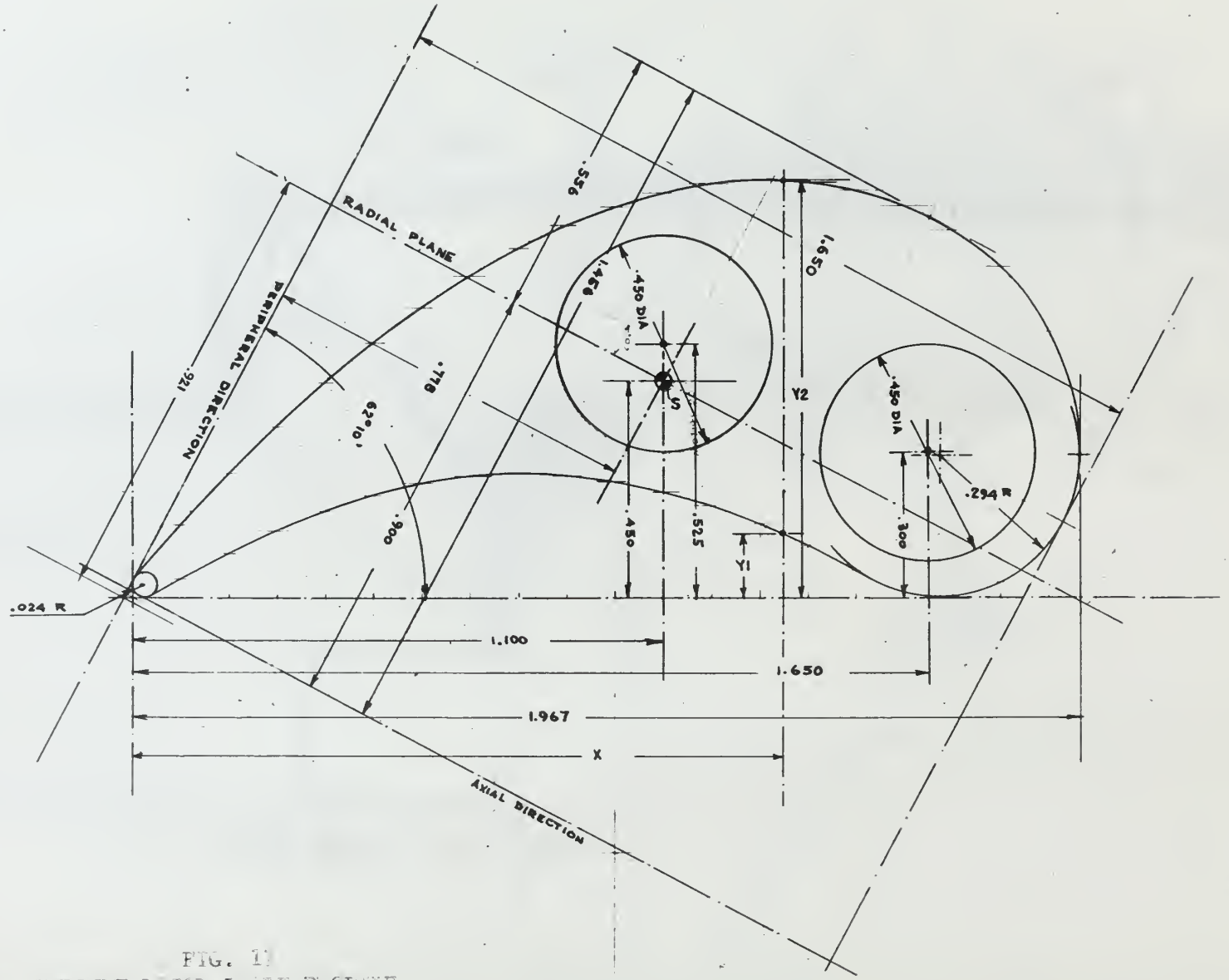

FIG. 1
TURBINE ROTOR BLADE PROFILE

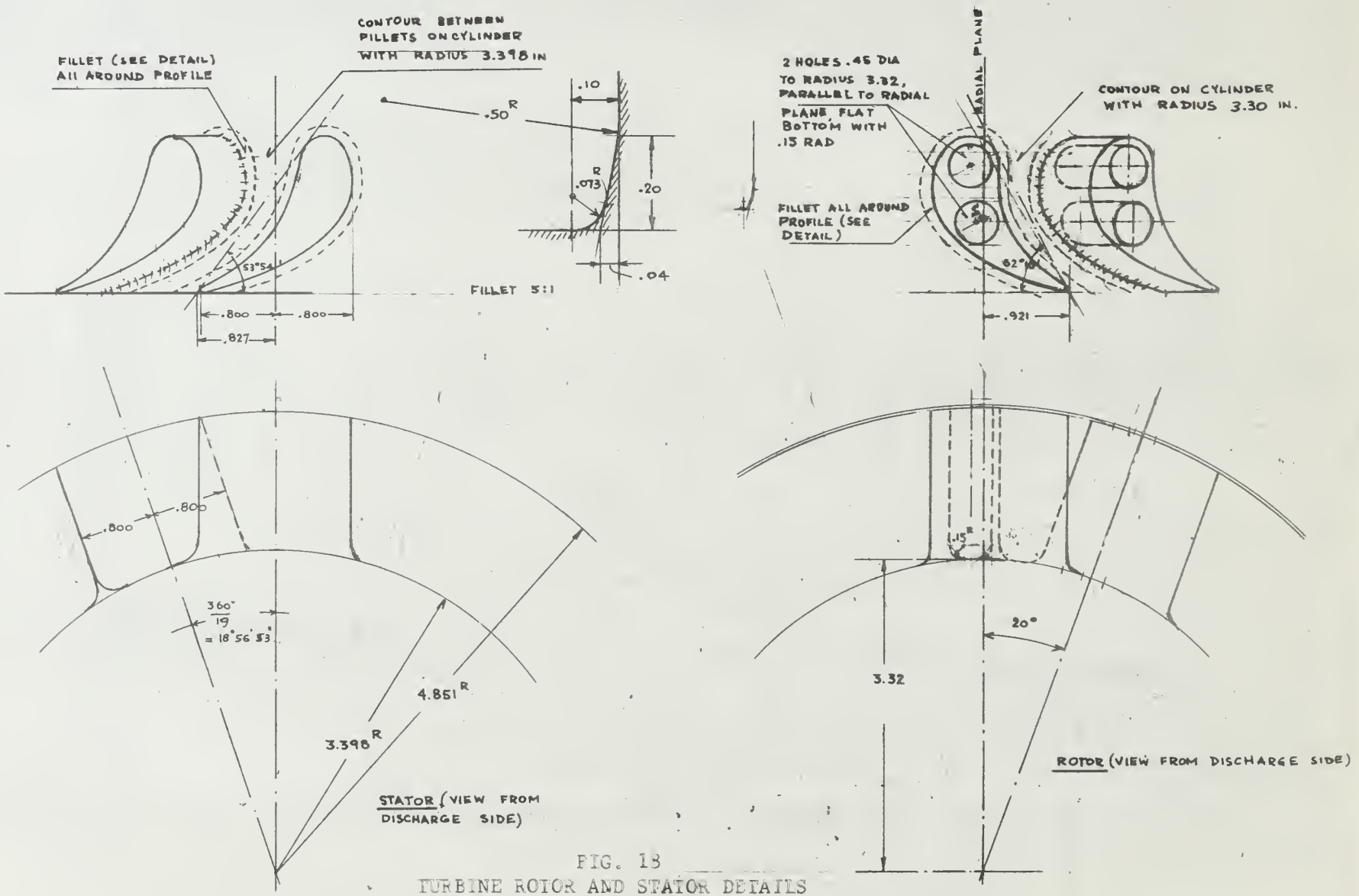

FIG. 13
TURBINE ROTOR AND STATOR DETAILS

FIG 19

FLOW NOZZLE COEFFICIENT. TURBINE TEST RIG

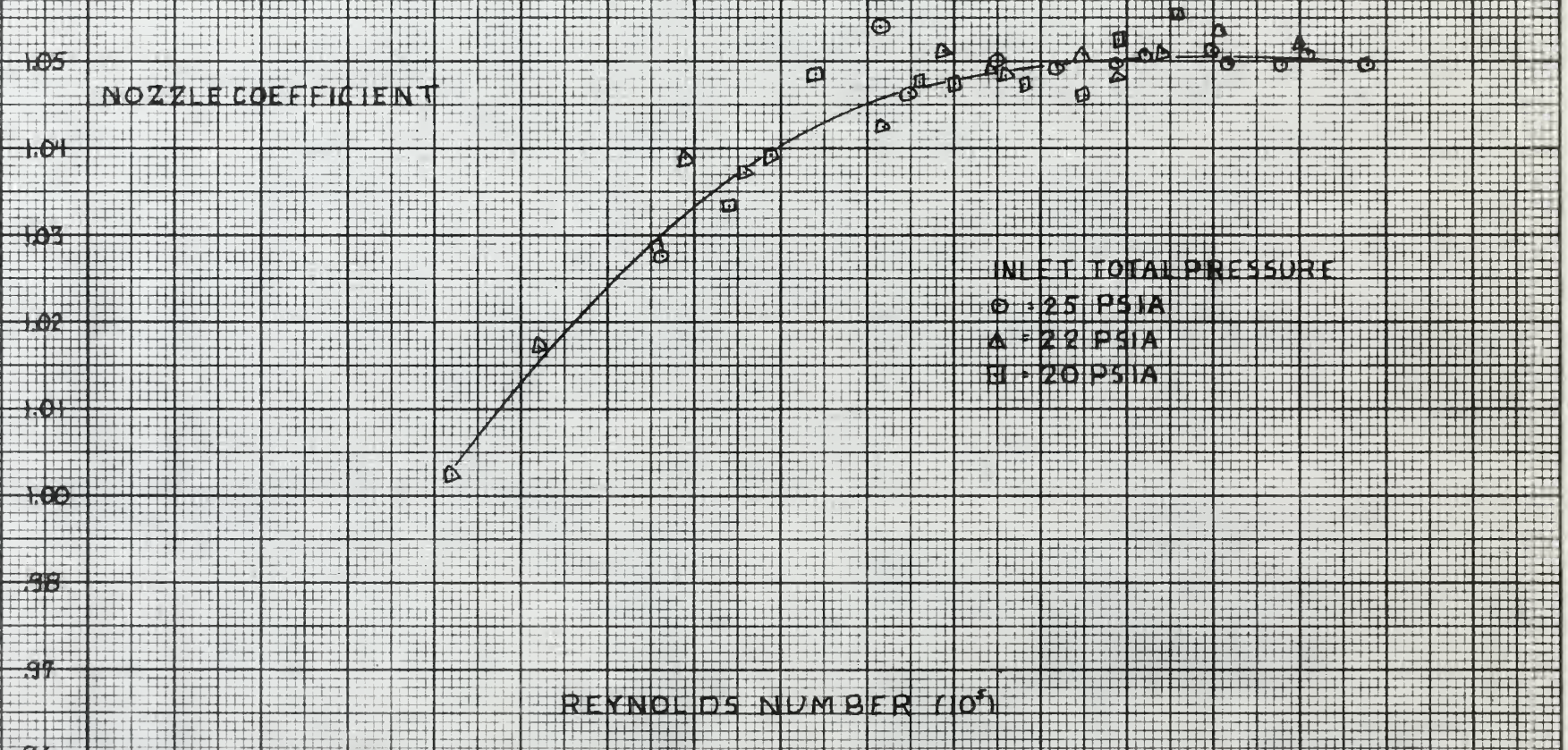

FIG 20

HORSEPOWER, ARES MOD II TURBINE

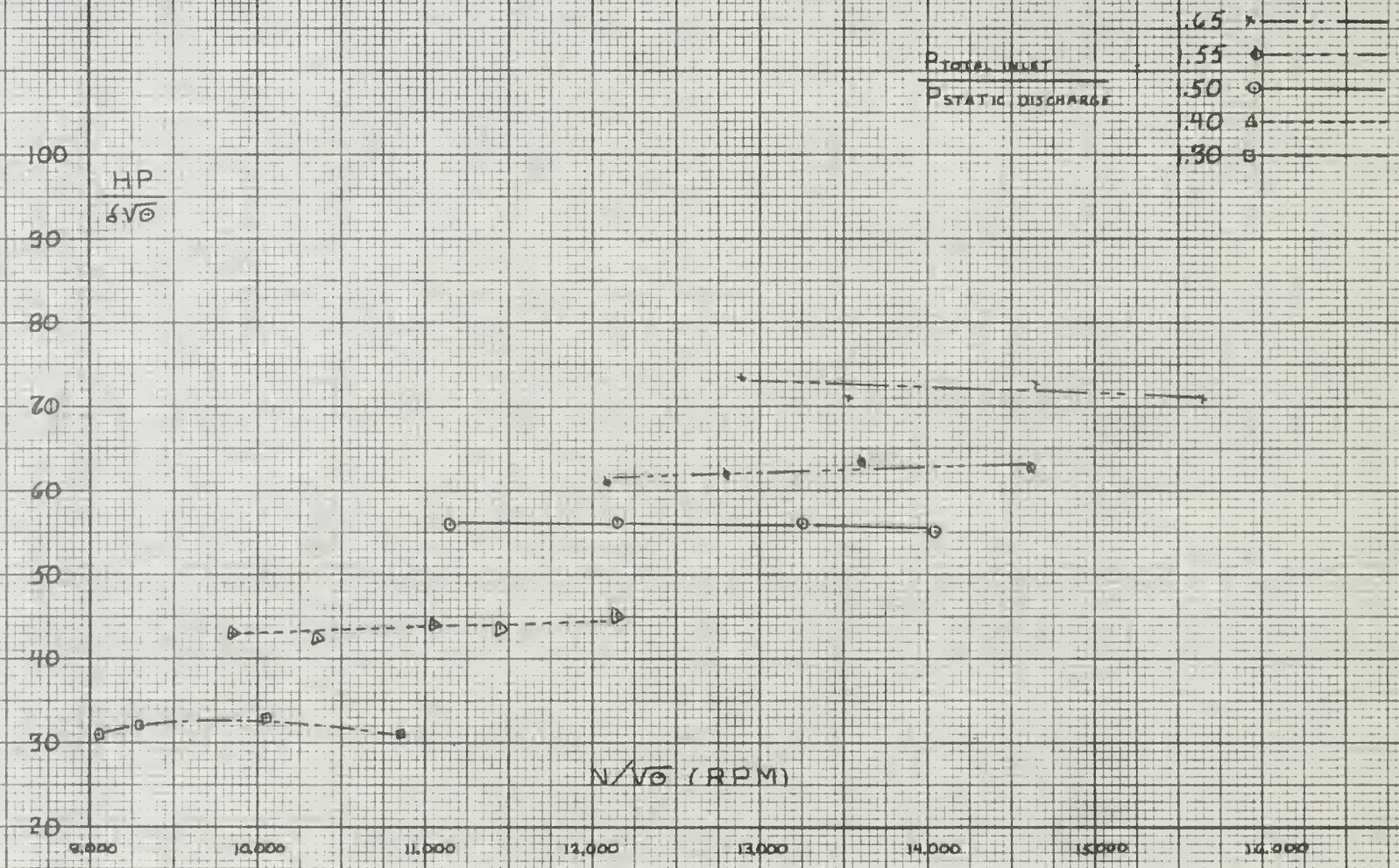

FIG 21

MOMENT ARES MOD II TURBINE

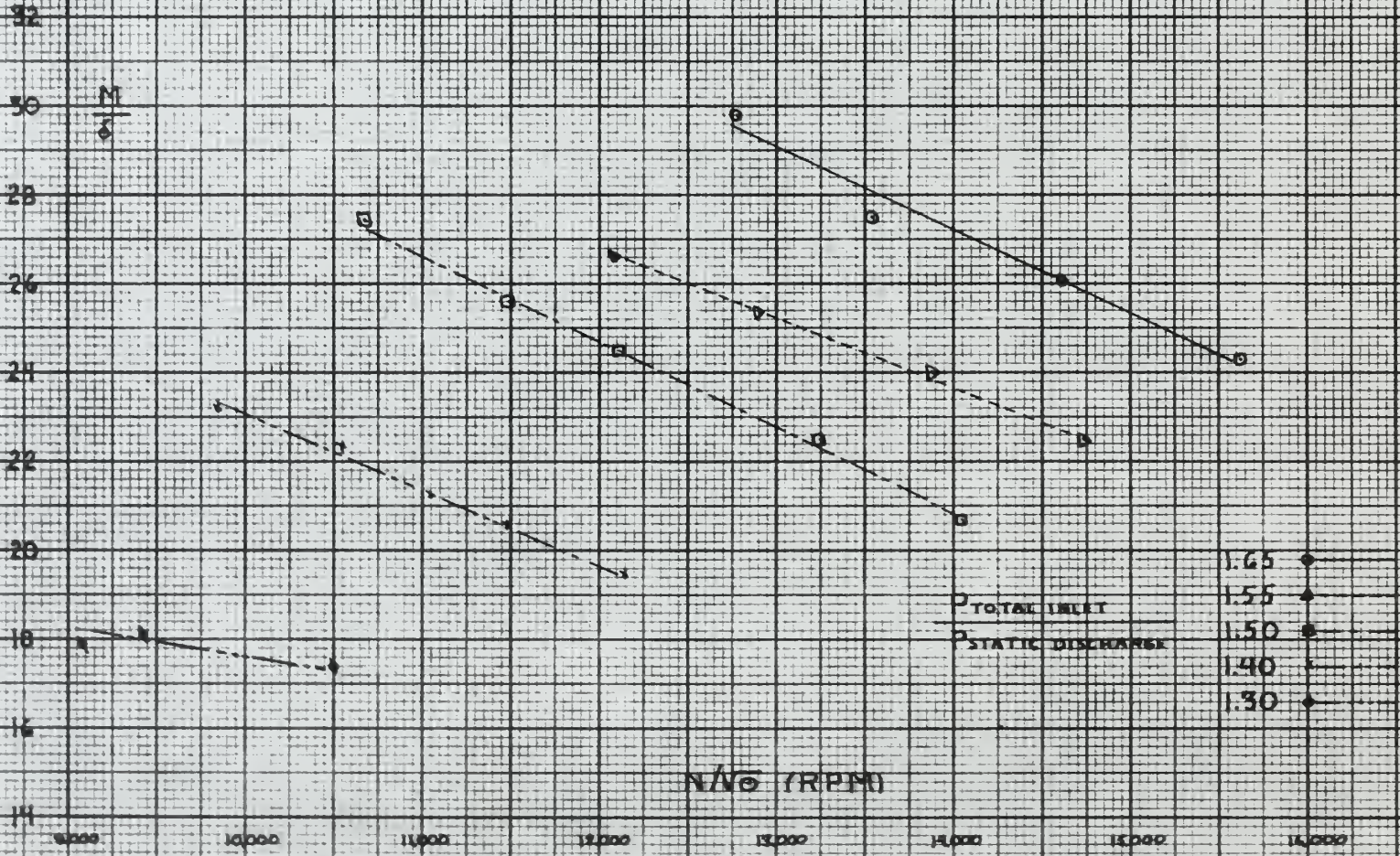

FIG 22

FLOW RATES, AIRES MOD II TURBINE

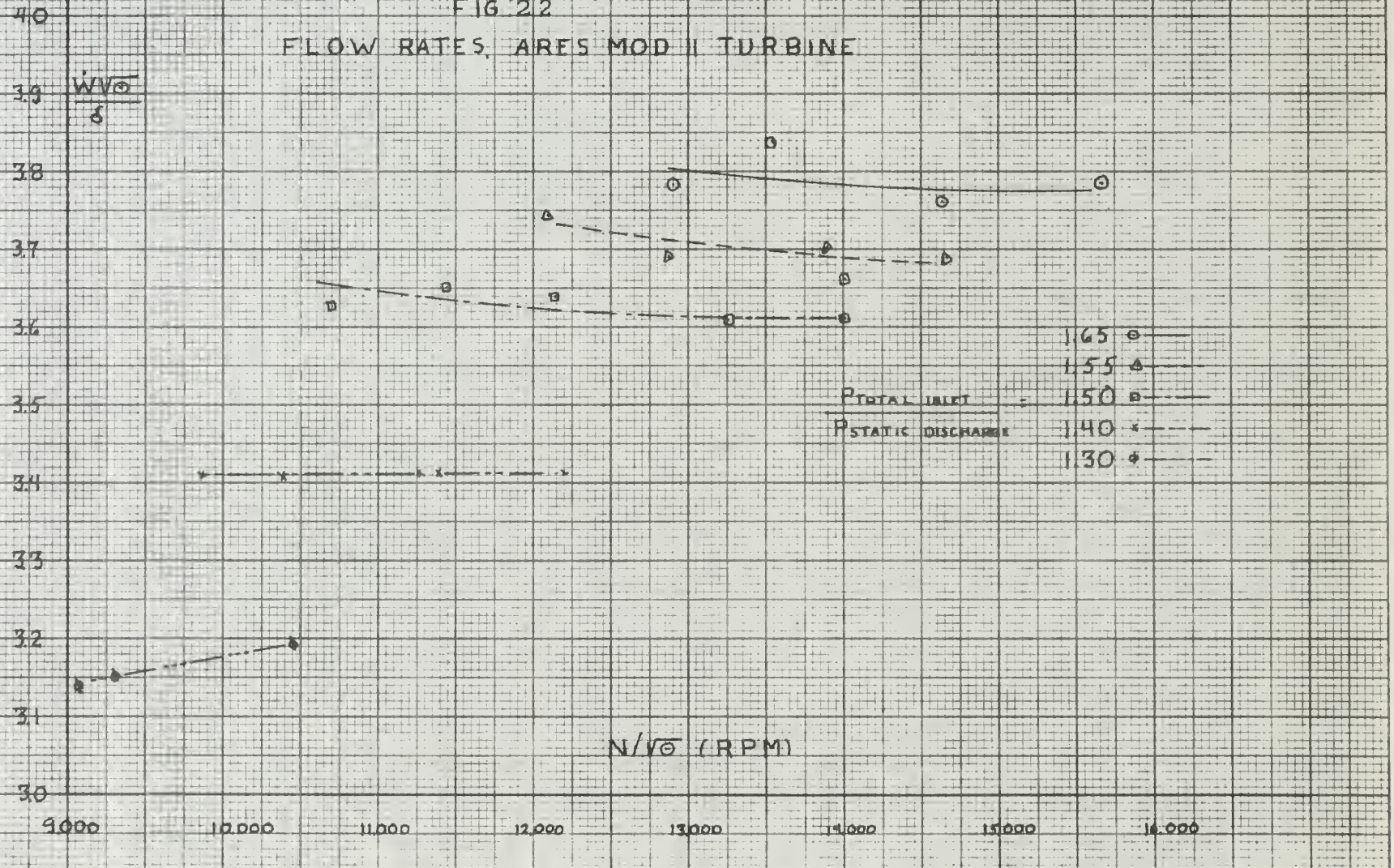

FIG 23

EFFICIENCY TESTS ARES MOD I TURBINE

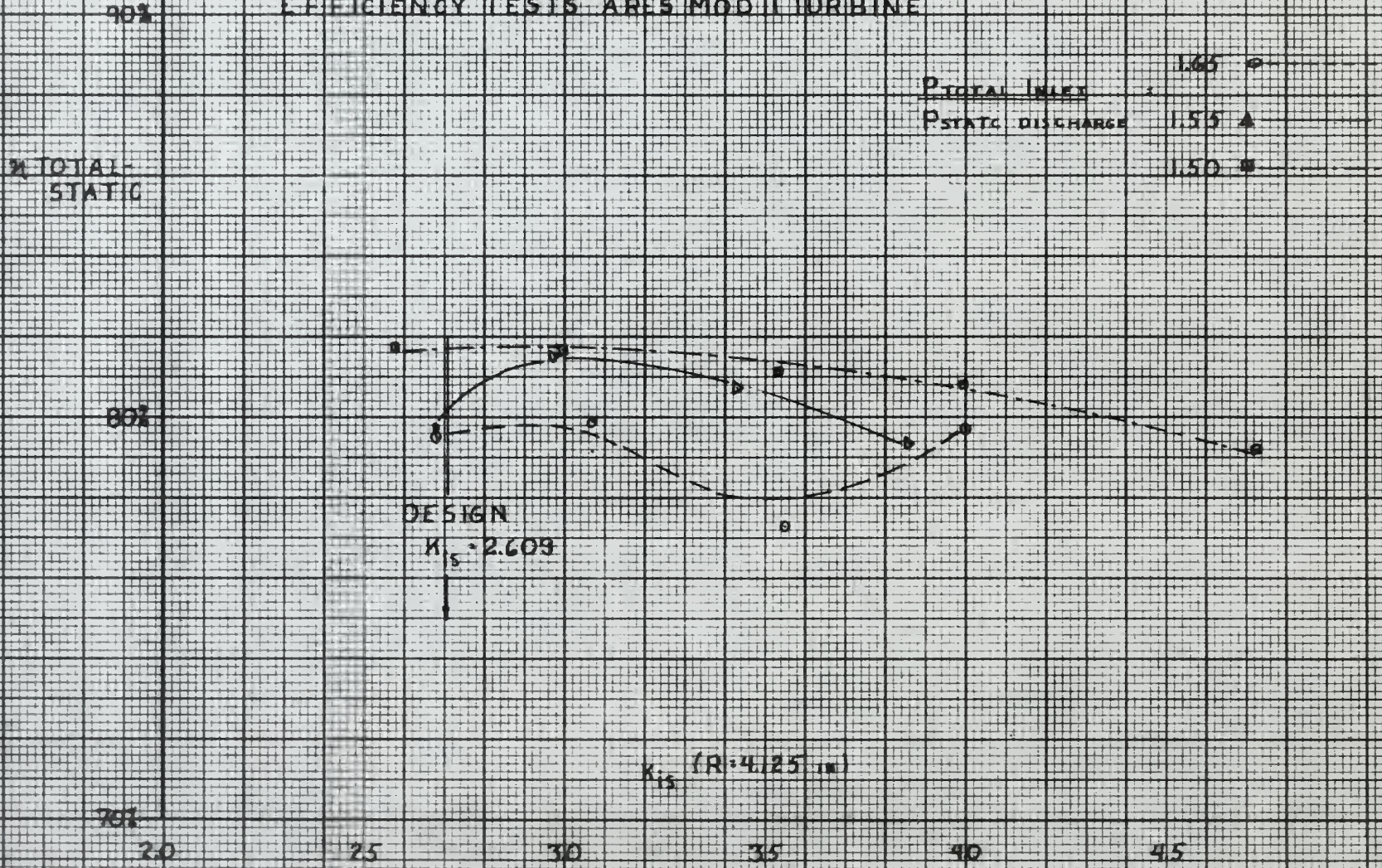

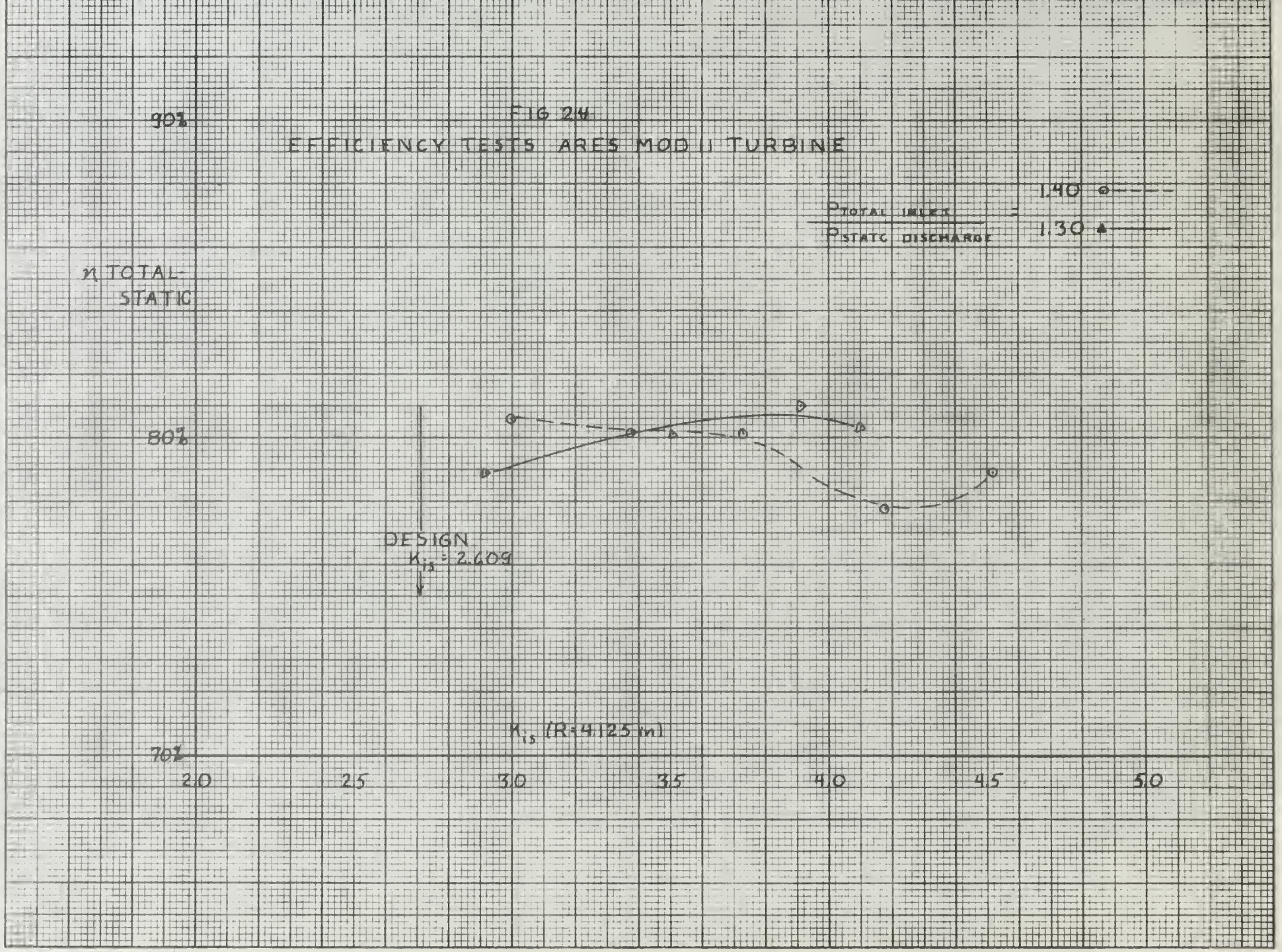
FIG 24
EFFICIENCY TESTS ARES MOD II TURBINE
$P_{TOTAL\ INLET}$ / $P_{STATIC\ DISCHARGE}$ = 1.40
1.30
η TOTAL-STATIC
90%
80%
70%
DESIGN
K_{is} = 2.609
K_{is} (R=4.125 in)
2.0
2.5
3.0
3.5
4.0
4.5
5.0

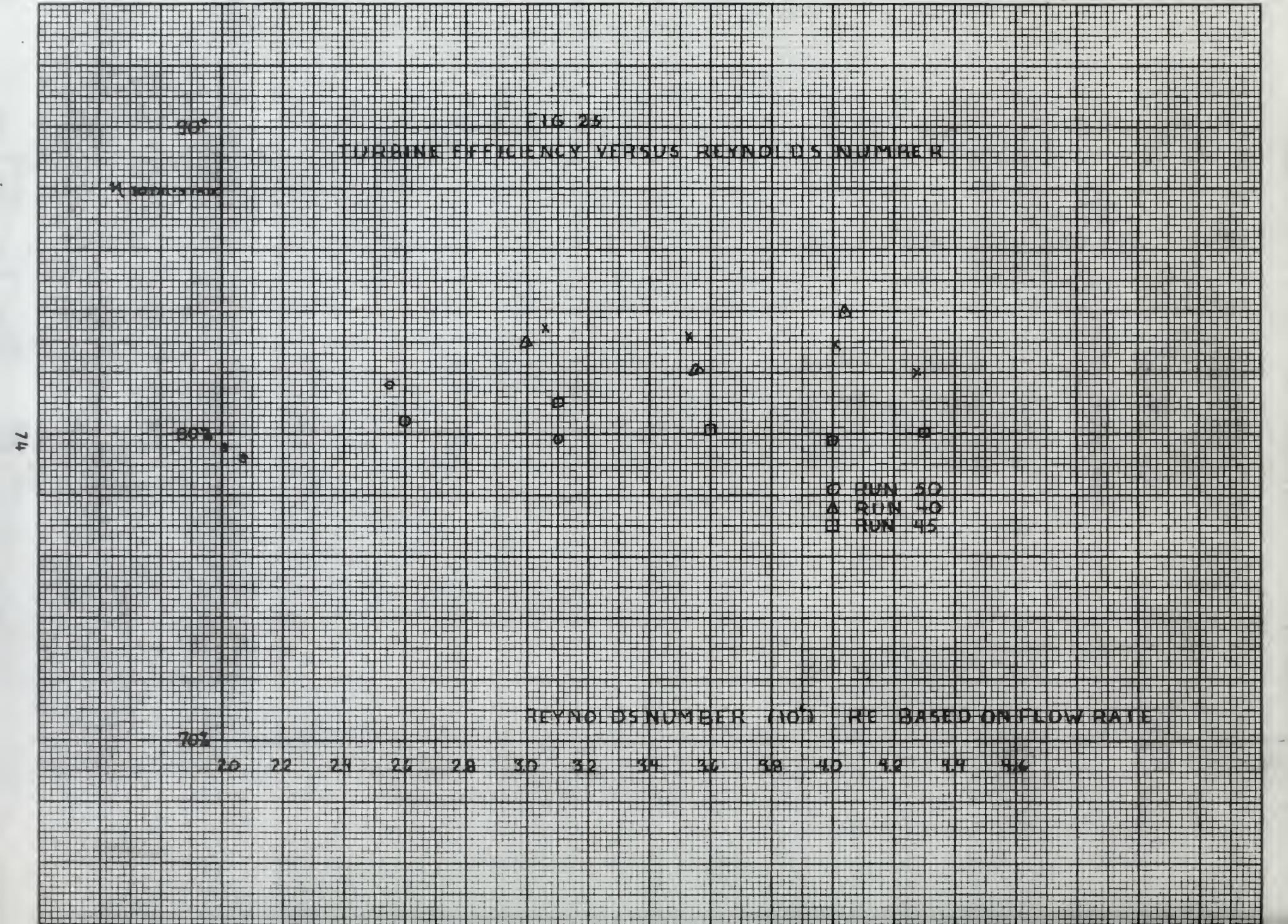
FIG 25
TURBINE EFFICIENCY VERSUS REYNOLDS NUMBER
30%
80%
70%
O RUN 50
Δ RUN 70
□ RUN 95
REYNOLDS NUMBER (10⁵) RE BASED ON FLOW RATE
2.0
2.2
2.4
2.6
2.8
3.0
3.2
3.4
3.6
3.8
4.0
4.2
4.4
4.6

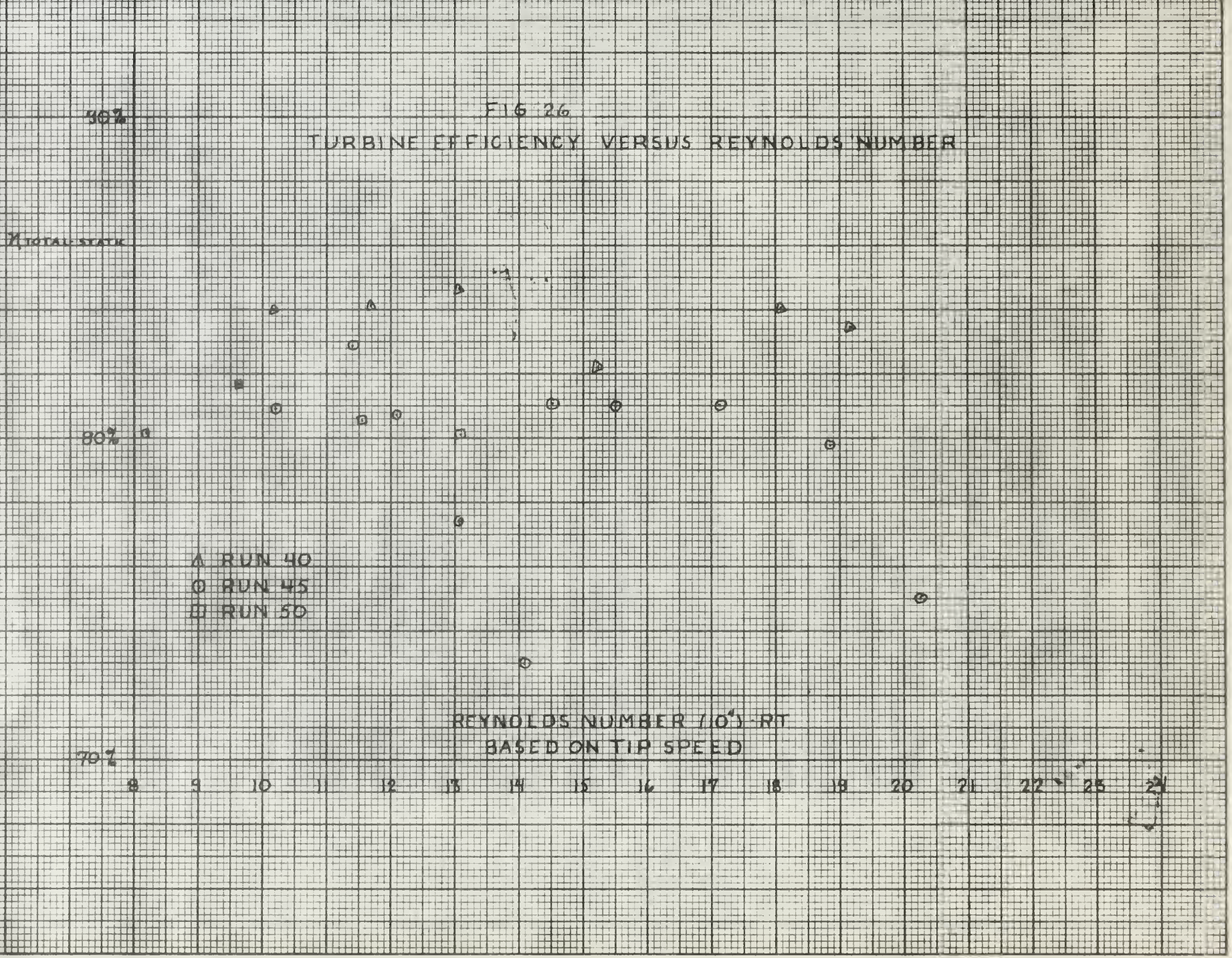
FIG 26
TURBINE EFFICIENCY VERSUS REYNOLDS NUMBER
η TOTAL-STATIC
90%
80%
70%
Δ RUN 40
○ RUN 45
□ RUN 50
REYNOLDS NUMBER (10⁴) RT
BASED ON TIP SPEED
8
9
10
11
12
13
14
15
16
17
18
19
20
21
22
23
24

INITIAL DISTRIBUTION LIST

		No Copies
1.	Defense Documentation Center Cameron Station Alexandria, Virginia 22314	20
2.	Library U.S. Naval Postgraduate School Monterey, California	2
3.	Commander Naval Air Systems Command Department of the Navy Washington, D. C. 20360	1
4.	Commandant of the Marine Corps (Code AO3C) Headquarters, U.S. Marine Corps Washington, D. C. 22214	1
5.	Chairman Department of Aeronautics U.S. Naval Postgraduate School Monterey, California 93940	1
6.	Prof. Michael H. Vavra (Thesis Advisor) Department of Aeronautics U.S. Naval Postgraduate School Monterey, California 93940	3
7.	CAPT Jacques Calvert Naviaux 3rd Marine Air Wing MCAS El Toro (Santa Ana), California	1
8.	Associate Prof. Roy Reichenbach Department of Aeronautics U.S. Naval Postgraduate School Monterey, California 93940	1
9.	Office of Naval Research (Power Branch) Department of the Navy Washington, D.C. 20360 (Attn: Mr. J. K. Patton, Jr.)	1

DOCUMENT CONTROL DATA - R&D

(Security classification of title, body of abstract and indexing annotation must be entered when the overall report is classified)

1 ORIGINATING ACTIVITY *(Corporate author)*

Naval Postgraduate School
Monterey, California 93940

2a. REPORT SECURITY CLASSIFICATION
UNCLASSIFIED

2b GROUP

3. REPORT TITLE

TRANSONIC TURBINE TEST RIG EXHAUSTER SYSTEM TESTS AND TESTS OF A REACTION TURBINE

4. DESCRIPTIVE NOTES *(Type of report and inclusive dates)*

Thesis, M.S., December 1966

5. AUTHOR(S) *(Last name, first name, initial)*

6. REPORT DATE	7a. TOTAL NO. OF PAGES	7b. NO. OF REFS
December 1966	78	15

8a. CONTRACT OR GRANT NO.	9a. ORIGINATOR'S REPORT NUMBER(S)
b. PROJECT NO.	
c.	9b. OTHER REPORT NO(S) *(Any other numbers that may be assigned this report)*
d.	

10. AVAILABILITY/LIMITATION NOTICES

This document has been approved for public release and sale; its distribution is unlimited.

Qualified requesters may obtain copies of this report from DDC.

B. Newberry 3/22/69

11. SUPPLEMENTARY NOTES	12. SPONSORING MILITARY ACTIVITY
	Commander Naval Air Systems Command Department of the Navy Washington, D. C. 20360

13 ABSTRACT

The primary purpose of the Exhauster System of the Transonic Turbine Test Rig of the United States Naval Postgraduate School, Monterey, California, is to increase the range of turbine operating pressure ratios by maintaining a partial vacuum inside a hood that encloses the turbine. The first part of this study is concerned with the design and the tests of the exhauster system. The experiments were used to establish a method of predicting the operating characteristics of similar ejectors which is based on the universal ejection properties of turbulent jets.

The second part of this study describes turbine tests utilizing the exhauster system that were carried out to investigate the effects of high values of the isentropic head coefficient and Reynolds number on the turbine performance. No correlation could be established between turbine Reynolds number and performance in the range tested.

DD FORM 1 JAN 64 1473

14. KEY WORDS	LINK A		LINK B		LINK C	
	ROLE	WT	ROLE	WT	ROLE	WT
Turbulent Jet Supersonic Ejector Reaction Turbine Reynolds Number						

INSTRUCTIONS

1. ORIGINATING ACTIVITY: Enter the name and address of the contractor, subcontractor, grantee, Department of Defense activity or other organization *(corporate author)* issuing the report.

2a. REPORT SECURITY CLASSIFICATION: Enter the overall security classification of the report. Indicate whether "Restricted Data" is included. Marking is to be in accordance with appropriate security regulations.

2b. GROUP: Automatic downgrading is specified in DoD Directive 5200.10 and Armed Forces Industrial Manual. Enter the group number. Also, when applicable, show that optional markings have been used for Group 3 and Group 4 as authorized.

3. REPORT TITLE: Enter the complete report title in all capital letters. Titles in all cases should be unclassified. If a meaningful title cannot be selected without classification, show title classification in all capitals in parenthesis immediately following the title.

4. DESCRIPTIVE NOTES: If appropriate, enter the type of report, e.g., interim, progress, summary, annual, or final. Give the inclusive dates when a specific reporting period is covered.

5. AUTHOR(S): Enter the name(s) of author(s) as shown on or in the report. Enter last name, first name, middle initial. If military, show rank and branch of service. The name of the principal author is an absolute minimum requirement.

6. REPORT DATE: Enter the date of the report as day, month, year; or month, year. If more than one date appears on the report, use date of publication.

7a. TOTAL NUMBER OF PAGES: The total page count should follow normal pagination procedures, i.e., enter the number of pages containing information.

7b. NUMBER OF REFERENCES: Enter the total number of references cited in the report.

8a. CONTRACT OR GRANT NUMBER: If appropriate, enter the applicable number of the contract or grant under which the report was written.

8b, 8c, & 8d. PROJECT NUMBER: Enter the appropriate military department identification, such as project number, subproject number, system numbers, task number, etc.

9a. ORIGINATOR'S REPORT NUMBER(S): Enter the official report number by which the document will be identified and controlled by the originating activity. This number must be unique to this report.

9b. OTHER REPORT NUMBER(S): If the report has been assigned any other report numbers *(either by the originator or by the sponsor)*, also enter this number(s).

10. AVAILABILITY/LIMITATION NOTICES: Enter any limitations on further dissemination of the report, other than those imposed by security classification, using standard statements such as:

(1) "Qualified requesters may obtain copies of this report from DDC."

(2) "Foreign announcement and dissemination of this report by DDC is not authorized."

(3) "U. S. Government agencies may obtain copies of this report directly from DDC. Other qualified DDC users shall request through _____."

(4) "U. S. military agencies may obtain copies of this report directly from DDC. Other qualified users shall request through _____."

(5) "All distribution of this report is controlled. Qualified DDC users shall request through _____."

If the report has been furnished to the Office of Technical Services, Department of Commerce, for sale to the public, indicate this fact and enter the price, if known.

11. SUPPLEMENTARY NOTES: Use for additional explanatory notes.

12. SPONSORING MILITARY ACTIVITY: Enter the name of the departmental project office or laboratory sponsoring *(paying for)* the research and development. Include address.

13. ABSTRACT: Enter an abstract giving a brief and factual summary of the document indicative of the report, even though it may also appear elsewhere in the body of the technical report. If additional space is required, a continuation sheet shall be attached.

It is highly desirable that the abstract of classified reports be unclassified. Each paragraph of the abstract shall end with an indication of the military security classification of the information in the paragraph, represented as *(TS), (S), (C), or (U)*.

There is no limitation on the length of the abstract. However, the suggested length is from 150 to 225 words.

14. KEY WORDS: Key words are technically meaningful terms or short phrases that characterize a report and may be used as index entries for cataloging the report. Key words must be selected so that no security classification is required. Identifiers, such as equipment model designation, trade name, military project code name, geographic location, may be used as key words but will be followed by an indication of technical context. The assignment of links, roles, and weights is optional.

DD FORM 1 JAN 64 1473 (BACK)